NASA TECHNICAL NOTE

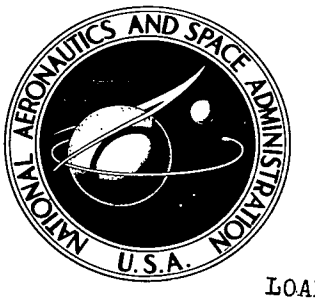

MODAL DENSITY ESTIMATES FOR SANDWICH PANELS: THEORY AND EXPERIMENT

by Larry L. Erickson

Ames Research Center

Moffett Field, Calif. 94035

NATIONAL AERONAUTICS AND SPACE ADMINISTRATION • WASHINGTON, D. C. • SEPTEMBER 1970

1. Report No. NASA TN D-5771	2. Government Accession No.	3. Recipient's Catalog No.
4. Title and Subtitle MODAL DENSITY ESTIMATES FOR SANDWICH PANELS: THEORY AND EXPERIMENT		5. Report Date September 1970 6. Performing Organization Code
7. Author(s) Larry L. Erickson		8. Performing Organization Report No. A-3106
9. Performing Organization Name and Address NASA Ames Research Center Moffett Field, Calif., 94035		10. Work Unit No. 124-08-05-08-00-21 11. Contract or Grant No.
12. Sponsoring Agency Name and Address National Aeronautics and Space Administration Washington, D.C. 20546		13. Type of Report and Period Covered Technical Note 14. Sponsoring Agency Code

15. Supplementary Notes

16. Abstract

Formulas are presented that can be used to estimate the average modal densities of sandwich beams and flat or cylindrically curved sandwich panels. Numerical results, presented in terms of general parameters, indicate the relative importance of transverse shear flexibility, orthotropic shear moduli of the core, face bending stiffness, rotary inertia, and panel curvature over a wide frequency range. Modal densities determined experimentally from resonance tests of flat rectangular sandwich panels having orthotropic cores are close to the modal densities estimated by theory except at frequencies near that of the fundamental mode. In this low-frequency range the theoretical estimates are not valid.

17. Key Words Suggested by author(s) Modal density Sandwich panels Vibration	18. Distribution Statement Unclassified - Unlimited		
19. Security Classif. (of this report) Unclassified	20. Security Classif. (of this page) Unclassified	21. No. of Pages 50	22. Price* $3.00

*For sale by the Clearinghouse for Federal Scientific and Technical Information
Springfield, Virginia 22151

SYMBOLS

a	axial length of panel, in. (m)
b	circumferential width of panel, in. (m)
C	curvature parameter, $\frac{1}{R}\frac{b^2}{\pi^2}\sqrt{\frac{E'}{D_s}}$
C_{eff}	effective curvature parameter defined by equation (28b)
d_1, d_2	distances from middle surface of top and bottom face sheets, respectively, to axis of rotation, in. (m) (see fig. 1), $\frac{E_{f_2} t_{f_2}}{E'} h_c \left(1 + \frac{t_{f_1} + t_{f_2}}{2h_c}\right)$, $\frac{E_{f_1} t_{f_1}}{E'} h_c \left(1 + \frac{t_{f_1} + t_{f_2}}{2h_c}\right)$
D_{f_1}, D_{f_2}	bending stiffnesses of top and bottom face sheets, respectively, in.-lbf (m-N) (See appendix A)
D_s	bending stiffness of panel, in.-lbf (m-N) (see appendix A)
D_Q	transverse shear stiffness for isotropic panel, lbf/in. (N/m) $G_c h_c \left(1 + \frac{t_{f_1} + t_{f_2}}{2h_c}\right)^2$
D_{Q_x}, D_{Q_y}	orthotropic transverse shear stiffnesses in x and y directions, respectively, lbf/in. (N-m) (see appendix A)
$D_{Q_{eff}} = \sqrt{D_{Q_x} D_{Q_y}}$	lbf/in. (N/m)
e	distance from middle surface of core to axis of rotation, in. (m) (see fig. 1), $d_1 - \frac{1}{2}\left(h_c + t_{f_1}\right)$
E_{f_1}, E_{f_2}	Young's modulus for top and bottom face sheets, respectively, lbf/in.^{2} (N/m^2)
E'	extensional stiffness of panel, lbf/in. (N/m) (see appendix A)
F	incomplete elliptic integral of the first kind
G_s	shear modulus of material from which core of sandwich panel is fabricated, lbf/in.^{2} (N/m^2)
G_{c_x}, G_{c_y}	orthotropic shear moduli of sandwich core in x and y directions, respectively, lbf/in.^{2} (N/m^2)

G_{L_D}, G_{L_F}, G_T theoretical shear moduli of a honeycomb core defined by equations (33), lbf/in.^{2} (N/m^2)

h_c thickness of sandwich core, in. (m)

I mass density moment of inertia, per unit width, about axis of rotation, lbf-sec^2/in. (kg) (see appendix A)

k modulus of K defined by equation (32)

k_1, k_2 moduli of F defined by equations (21a) and (21b), respectively

K complete elliptic integral of the first kind

m,n integers giving number of half-waves in x and y directions, respectively

M mass density per unit area of panel, lbf-sec^2/in.^{3} (kg/m^2) (see appendix A)

M_x, M_y bending moments, per unit width, acting on cross sections originally perpendicular to the x and y axes, respectively, in.-lbf/in. (m-N/m)

N cumulative number of modes occurring below a specified frequency

Q_x, Q_y resultant shearing forces, per unit width, acting in z direction in planes originally parallel to the yz and xz planes, respectively, lbf/in. (N/m)

R constant radius of curvature of panel, in. (m)

r shear flexibility parameter for isotropic panel, $\frac{\pi^2}{b^2}\frac{D_s}{D_Q}$

r_x, r_y orthotropic shear flexibility parameters of a sandwich panel in x and y directions, respectively, $\frac{\pi^2}{b^2}\frac{D_s}{D_{Q_x}}$, $\frac{\pi^2}{b^2}\frac{D_s}{D_{Q_y}}$

$r_{eff} = \frac{\pi^2}{b^2}\frac{D_s}{D_{Q_{eff}}}$

S surface area of panel, in.^{2} (m^2)

t time, sec

t_{f_1}, t_{f_2} thicknesses of top and bottom face sheets, respectively, in. (m)

u,v wall dimensions of honeycomb cell, in. (m)

w deflection of panel, measured in z direction, in. (m)

x,y,z orthogonal coordinates, in. (m) (see fig. 1)

$\alpha = 1 - \left(\frac{C}{\omega/\omega_o}\right)^2 \cos^4(\theta)$

β quantity defined by equation (32)

$\delta^2 = \frac{\tau(2rC)^2}{1 + \tau[2r(\omega/\omega_o)]^2}$

$\gamma = \frac{D_{Q_x}}{D_{Q_y}} = \frac{G_{c_x}}{G_{c_y}}$

ΔN the number of modes occurring in a frequency band $\Delta\omega$

ζ quantity defined by equation (3b)

η cell angle of honeycomb, deg

θ $\tan^{-1} \frac{n}{m/(a/b)}$

μ Poisson's ratio of face sheets

$\rho^2 = \left(\frac{m}{a/b}\right)^2 + n^2$

ρ_c mass density of core, lbf-sec^2/in.^{4} (kg/m^3)

ρ_{f_1}, ρ_{f_2} mass densities of top and bottom face sheets, respectively, lbf-sec^2/in.^{4} (kg/m^3)

ρ_s mass density of material from which core of sandwich panel is fabricated, lbf-sec^2/in.^{4} (kg/m^3)

$\rho_{f_{eff}}$ "effective" mass density of faces obtained by lumping bonding material mass with the face sheet mass, lbf-sec^2/in.^{4} (kg/m^3)

$\tau = \frac{D_{f_1} + D_{f_2}}{D_s}$

ϕ_1, ϕ_2 amplitudes of F defined by equations (21a) and (21b), respectively

χ rotary inertia parameter, $\frac{\pi^2}{b^2}\frac{I}{M}$

ω	frequency, rad/sec
ω_o	fundamental frequency of a semi-infinite, simply supported panel of length b, as predicted by classical plate theory, rad/sec, $\frac{\pi^2}{b^2}\sqrt{\frac{D_s}{M}}$

Subscripts

f_1, f_2	top and bottom face sheets, respectively
c	core of sandwich panel
eff	effective value or quantity

MODAL DENSITY ESTIMATES FOR SANDWICH PANELS: THEORY AND EXPERIMENT[1]

Larry L. Erickson

Ames Research Center

SUMMARY

Formulas are presented that can be used to estimate the average modal densities of sandwich beams and flat or cylindrically curved sandwich panels. Numerical results, presented in terms of general parameters, indicate the relative importance of transverse shear flexibility, orthotropic shear moduli of the core, face bending stiffness, rotary inertia, and panel curvature over a wide frequency range. Modal densities determined experimentally from resonance tests of flat rectangular sandwich panels having orthotropic cores are close to the modal densities estimated by theory except at frequencies near that of the fundamental mode. In this low-frequency range the theoretical estimates are not valid.

INTRODUCTION

Predicting the vibratory response of structures to random environmental loads that are distributed over a wide frequency range (e.g., rocket engine and turbulent boundary-layer noise) presents considerable difficulties. In the conventional approach to vibration analysis the response is expressed as a series, the terms of which involve the structure's free vibration mode shapes and resonance frequencies. Unfortunately, for most practical structures the mode shapes and resonance frequencies, especially those occurring at the higher frequencies, are difficult to obtain. As a consequence, there has been an effort during the past few years to develop a new approach to multimodal vibration problems that avoids the difficulties of expanding the response in terms of the mode shapes (see, e.g., refs. 1 and 2). In this approach, sometimes referred to as "statistical energy analysis," average response levels in various frequency bands are estimated without knowledge of the mode shapes and resonance frequencies. Instead, what is required is a knowledge of the type (e.g., flexural) and number of structural vibration modes occurring in a given frequency interval. The number of modes per unit frequency is called the "modal density" of the structure.

Because a structure's modal density is relatively independent of the boundary conditions, statistical energy analysis shows promise of becoming a

[1]Part of the information presented herein was published under the title "Modal Densities of Sandwich Panels: Theory and Experiment," in the Shock and Vibration Bulletin, Bull. 39, Pt. 3, U.S. Dept. of Defense, Jan. 1969, pp. 1-16.

useful analysis technique for estimating average response levels of multimodal structural vibrations. This approach has been used to study a number of practical vibration problems including launch vehicle response to acoustic pressure fields (refs. 3 and 4), noise vibration transmission in space vehicles (ref. 5), vibration transmission into an instrument package (ref. 6), and sound transmission through a partition (ref. 7). In each case, the modal densities of the structures were required in the analysis. For example, one of the more useful response quantities is acceleration spectral density, which is directly proportional to modal density.

Equations have been derived for the modal densities of several structural elements and can be found in references 8 and 9. A portion of the results in reference 9 pertains to flat and doubly curved sandwich panels, and it is shown there that the transverse shear flexibility of a panel can have a significant effect on the panel's modal density. However, the results of reference 9 apply only to sandwich panels with isotropic cores and whose faces behave as membranes (i.e., the face bending stiffness is neglected). Since the cores of lightweight sandwich panels often have shear orthotropy (e.g., honeycomb), there is a practical need for equations that account for the effect of core orthotropy on the modal density. In addition, it is known from sandwich-panel buckling theory that for small wavelengths of deformation the face bending stiffness can become important (ref. 10).

In the present investigation, modal density estimates are obtained analytically for sandwich beams and for flat or cylindrically curved sandwich panels. The effects of the core's transverse shear flexibility, including orthotropic shear moduli parallel to the faces, face bending stiffness, and rotary inertia, are examined. Numerical results are presented in graphic form.

In addition, experimental results obtained from resonance tests of flat rectangular sandwich panels having orthotropic honeycomb cores are presented. In these tests, up to 80 consecutive vibration modes per panel were excited and identified. The experimentally determined modal densities are compared with the modal densities predicted by theory.

THEORY AND ASSUMPTIONS

Panel

The structural elements considered are a flat or cylindrically curved sandwich panel and a sandwich beam. The coordinate system and geometry of the curved sandwich panel are shown in figure 1. The panel is of length a and circumferential width b, and has a constant radius of curvature R. Each face sheet is isotropic, homogeneous, and of uniform thickness. The thickness, Young's modulus, and mass density of the top face sheet may be different from the thickness, modulus, and density of the bottom face sheet. The core may possess orthotropic shear moduli (G_{c_x}, G_{c_y}) and is of uniform thickness h_c.

The modal density estimates obtained herein are based on three frequency equations that relate the panel natural frequencies (ω rad/sec) to various physical characteristics of the panel and to the number of half-waves m and n that form in the x and y directions, respectively. The first of these equations, which is derived from the theory of reference 11 (see appendix B), is

$$\left[\left(\frac{\omega}{\omega_o}\right)^2 - \left(\frac{C}{\rho^2}\right)^2\left(\frac{m}{a/b}\right)^4\right]\left(\left\{1 + r_x\left[\frac{1-\mu}{2}\rho^2 - \chi\left(\frac{\omega}{\omega_o}\right)^2\right]\right\}\left\{1 + r_y\left[\frac{1-\mu}{2}\rho^2 - \chi\left(\frac{\omega}{\omega_o}\right)^2\right]\right\}\right.$$

$$\left. + \left(\frac{1+\mu}{2}\right)\left\{\left[\frac{1-\mu}{2}\rho^2 - \chi\left(\frac{\omega}{\omega_o}\right)^2\right]r_x r_y \rho^2 + r_x\left(\frac{m}{a/b}\right)^2 + r_y n^2\right\}\right)$$

$$- \left[\rho^2 - \chi\left(\frac{\omega}{\omega_o}\right)^2\right]\left\{\rho^2 + \left[\frac{1-\mu}{2}\rho^2 - \chi\left(\frac{\omega}{\omega_o}\right)^2\right]\left[r_y\left(\frac{m}{a/b}\right)^2 + r_x n^2\right]\right\} = 0 \qquad (1)$$

where $\rho^2 = [m/(a/b)]^2 + n^2$. In this equation, the physical and geometric properties of the panel are described by the following dimensionless quantities:

1. The length-width ratio a/b

2. The curvature parameter C, which is proportional to $1/R$

3. The rotary inertia parameter χ, which is proportional to the panel's mass density moment of inertia

4. The shear flexibility parameters r_x and r_y, which are proportional to $1/G_{c_x}$ and $1/G_{c_y}$, respectively

The reference frequency ω_o is the fundamental frequency of a flat, simply supported, semi-infinite sandwich panel with length b ($a/b = \infty$) as predicted by classical plate theory (shear and rotary inertia neglected); μ is Poisson's ratio of the faces and is assumed to be the same for both faces.

In equation (1), the bending stiffness of the faces about their own middle surface has been neglected. The second frequency equation accounts for the face bending stiffness but does not incorporate the effects of rotary inertia or curvature. This equation, obtained from reference 12 is

$$\left(\frac{\omega}{\omega_o}\right)^2 = \left[\left(\frac{m}{a/b}\right)^2 + n^2\right]^2\left(\tau + \frac{1}{1+\zeta}\right) \qquad (2)$$

where τ is the ratio of the sum of the face bending stiffnesses to the panel

bending stiffness. For identical faces of thickness $t_f = t_{f_1} = t_{f_2}$, τ becomes simply

$$\tau = \frac{1}{3}\left(\frac{t_f/h_c}{1 + t_f/h_c}\right)^2 \tag{3a}$$

The quantity ζ is due to the orthotropic shear flexibilities of the core, characterized by the ratio $\gamma = G_{c_x}/G_{c_y}$, and is given by

$$\zeta = \frac{r_y}{\gamma}\left[\left(\frac{m}{\frac{a}{b}}\right)^2 + \gamma n^2\right] \frac{1 + \left(\frac{1-\mu}{2}\right) r_y \frac{\left[\left(\frac{m}{a/b}\right)^2 + n^2\right]^2}{\left(\frac{m}{a/b}\right)^2 + \gamma n^2}}{1 + \left(\frac{1-\mu}{2}\right) r_y \left[\left(\frac{m}{a/b}\right)^2 + \frac{n^2}{\gamma}\right]} \tag{3b}$$

The third frequency equation accounts for both the face bending stiffness and panel curvature but does not incorporate the effects of rotary inertia or orthotropic shear moduli of the core. This equation, obtained from the curved panel buckling solution of reference 10, is

$$\left(\frac{\omega}{\omega_o}\right)^2 = \left[\left(\frac{m}{a/b}\right)^2 + n^2\right]^2 \left(\tau + \frac{1}{1 + r\{[m/(a/b)]^2 + n^2\}}\right) + \frac{C^2[m/(a/b)]^4}{\{[m/(a/b)]^2 + n^2\}^2} \tag{4}$$

Note: The last term in equations (11) and (13) of reference 10 contains a misprint, which has been corrected in equation (4)[2] above.

It should be noted that equations (1), (2), and (4) are consistent. Equations (1) and (2) are identical when the effects of rotary inertia, curvature, and face bending stiffness are simultaneously neglected ($\chi = C = \tau = 0$). Equations (1) and (4) are identical in the case of an isotropic core ($r_x = r_y = r$) when rotary inertia and the face bending stiffness are simultaneously neglected ($\chi = \tau = 0$). Equations (2) and (4) are identical in the case of an isotropic core ($r_x = r_y = r$, $\gamma = 1$) when the panel curvature is neglected ($C = 0$).

The basic assumptions made in the theories on which equations (1), (2), and (4) are based are:

1. Core and faces show linear, elastic behavior.

2. The transverse deflection of the panel comprises deformations due to both transverse shearing forces and bending moments.

---

[2]The symbols C, r, and τ in this report are called Z_b/π^2, ψ_b, and S, respectively, in reference 10.

3. The bending stiffness of the core is negligible compared to the overall bending stiffness of the panel, allowing the panel's flexural deformations to be described by an isotropic bending stiffness D_s.

4. Axial and circumferential inertia loadings are neglected.

5. Transverse shear strains in the faces and all normal strains in the z direction are neglected.

6. The cores are homogeneous; thus, for cellular type cores such as honeycomb the wavelengths of vibration must be at least several times the cell size.

7. For the cylindrically curved panel, three additional assumptions are:

   a. The total panel thickness is small compared to the radius of curvature.

   b. The effect of the transverse shearing force Q_y is neglected in the equation of circumferential equilibrium.

   c. The moment-distortion (curvature) relations are the same as for the flat panel.

Although the natural frequencies predicted by equations (1), (2), and (4) are valid only for simply supported panels, the equations for modal density are applicable to panels having other boundary conditions: Once the frequency range of the lowest several modes is exceeded, the boundary conditions generally have a negligible effect on the number of modes existing in a given frequency interval. This has been observed experimentally for flat panels and cylindrical shells that were essentially rigid in shear (refs. 13, 14, and 15). For mathematical arguments, see references 16 and 17.

Modal Density Formulation

For a given panel configuration (a/b, C, χ, r_x, r_y, τ, μ, and ω_o fixed) equation (1), (2), or (4) represents a set of constant frequency curves in the m/(a/b), n plane. Figure 2 is a typical curve. Each combination of m and n represents the only mode that occurs in an area 1[1/(a/b)] in the first quadrant of the m/(a/b), n plane. The total area occupied by the N modes bounded by the curve ω/ω_o = constant is approximately N[1/(a/b)]. This area is also given, approximately, by $(1/2)\int_{\theta_1}^{\theta_2}\rho^2(\omega,\theta)d\theta$, where θ is defined in figure 2 and $\rho^2 = [m/(a/b)]^2 + n^2$ is determined in terms of ω and θ from equation (1), (2), or (4). The limits of integration are such that ρ^2 is real and positive in the region $0 \leq \theta \leq (\pi/2)$. As in reference 16, the approximate number of modes existing below the specified frequency ω = constant is then expected to be asymptotically equal to

$$N \simeq \frac{1}{2}\frac{a}{b}\int_{\theta_1}^{\theta_2}\rho^2(\omega,\theta)d\theta$$

The average number of modes ΔN existing in a frequency band $\Delta\omega$ about the center frequency ω defines the average modal density $\Delta N/\Delta\omega$. This, then, is approximated by

$$\frac{\Delta N}{\Delta\omega} \simeq \frac{dN}{d\omega} \simeq \frac{1}{2}\frac{a}{b}\left[\int_{\theta_1}^{\theta_2} \frac{\partial\rho^2(\omega,\theta)}{\partial\omega}\, d\theta + \rho^2(\omega,\theta_2)\frac{d\theta_2}{d\omega} - \rho^2(\omega,\theta_1)\frac{d\theta_1}{d\omega}\right]$$

where Leibnitz's rule has been used. For the panel configurations considered herein the last two terms in the above equation turn out to be zero.

If classical plate theory is used to predict the modal density of a flat sandwich panel, the frequency independent value $dN/d\omega \simeq (\pi/4)(a/b)(1/\omega_o)$ is obtained (ref. 17). On the basis of this theory, the modal density is seen to depend only on the panel's lateral dimensions, bending stiffness, and mass per unit area ($\omega_o = (\pi^2/b^2)\sqrt{D_s/M}$). For comparison with this classical plate theory value, the sandwich panel modal density estimates presented herein are all expressed in the dimensionless form

$$\frac{1}{(\pi/4)(a/b)}\frac{dN}{d(\omega/\omega_o)} \simeq \frac{2}{\pi}\int_{\theta_1}^{\theta_2} \frac{\partial\rho^2(\omega/\omega_o,\theta)}{\partial(\omega/\omega_o)}\, d\theta \qquad (5)$$

From the results that follow it can be noted that the right-hand side of equation (5) is independent of the panel length and width. These lateral dimensions appear only on the left-hand side of the equation, and since the term $(a/b)(1/\omega_o)$ is proportional to the product ab, the modal density $\Delta N/\Delta\omega$ is directly proportional to the surface area of the panel. Although equations (1), (2), and (4) were derived on the basis of a rectangular planform, the modal densities obtained from them should be applicable to panels with other shapes of surface area S by replacing the rectangular area ab with the area S (ref. 17).

ANALYSIS

To calculate the modal density from equation (5) requires that $\partial\rho^2/\partial(\omega/\omega_o)$ be expressed analytically as a function of ω and θ. Unfortunately, ρ^2 appears as a cubic term in equations (1) and (4) and as a quartic term in equation (2), and thus is not readily obtained analytically. However, for the isotropic core ($r_x = r_y = r$) equations (1) and (2) can be solved exactly for $\partial\rho^2/\partial(\omega/\omega_o)$. Also, for an isotropic core, equation (4) can be used to obtain an approximate solution giving the combined effect of shear flexibility, panel curvature, and face bending stiffness. This is done in the following sections. It is then shown, by neglecting the face bending stiffness, that the isotropic results can be applied to panels with moderately orthotropic cores if "effective" shear flexibility and curvature parameters are used. Finally, an approximate solution is obtained for a flat panel, which gives the combined effect of orthotropic shear moduli and face bending stiffness.

Flat Sandwich Panel With Isotropic Core

Face bending stiffness neglected- The frequency equation for this case is obtained from equation (1) by setting $C = 0$ and $r_x = r_y = r$, which results in two separate factors either of which is a solution if set equal to zero.

$$1 + r\left[\rho^2 \frac{1 - \mu}{2} - \chi\left(\frac{\omega}{\omega_o}\right)^2\right] = 0 \tag{6a}$$

$$\left(\frac{\omega}{\omega_o}\right)^2\left\{1 + r\left[\rho^2 - \chi\left(\frac{\omega}{\omega_o}\right)^2\right]\right\} - \rho^2\left[\rho^2 - \chi\left(\frac{\omega}{\omega_o}\right)^2\right] = 0 \tag{6b}$$

These equations are equivalent to those obtained in reference 18 and for a given value of ρ^2 yield three values of ω^2. The vibrations corresponding to the two higher frequencies, given by equation (6a) and the larger frequency root of equation (6b), are described in reference 18 as the thickness-twist and thickness-shear modes, respectively. The lower frequency vibration, given by the smaller frequency root of equation (6b), corresponds to a primarily flexural type of motion. This "bending set" of modes usually is of most interest in structural response problems and is described by

$$2\rho^2 = (r + \chi)\left(\frac{\omega}{\omega_o}\right)^2 + \sqrt{\left[(r + \chi)\left(\frac{\omega}{\omega_o}\right)^2\right]^2 + 4\left(\frac{\omega}{\omega_o}\right)^2\left[1 - r\chi\left(\frac{\omega}{\omega_o}\right)^2\right]} \tag{7}$$

Since ρ^2 is independent of θ (i.e., the curve ω = constant is a circle in the $m/(a/b)$, n plane), the limits of integration in equation (5) are $\theta_1 = 0$ and $\theta_2 = \pi/2$. Integration yields the following estimate for the modal density of a flat sandwich panel having an isotropic core:

$$\frac{1}{(\pi/4)(a/b)} \frac{dN}{d(\omega/\omega_o)} \simeq \left(1 + \frac{\chi}{r}\right)\left(r \frac{\omega}{\omega_o}\right) + \frac{1 + (1/2)[1 - (\chi/r)]^2[r(\omega/\omega_o)]^2}{\sqrt{1 + (1/4)[1 - (\chi/r)]^2[r(\omega/\omega_o)]^2}} \tag{8}$$

The variation in modal density with $r(\omega/\omega_o)$, as given by equation (8), is shown in figure 3 for $\chi/r = 0$ (i.e., rotary inertia neglected) and $\chi/r = 0.279$. For $r = 0$ (infinite shear stiffness) the frequency-independent, classical plate theory value for modal density is obtained. When shear flexibility is not neglected ($r > 0$), the modal density increases with increasing frequency and with increasing shear flexibility. The value $\chi/r = 0.279$ corresponds to the extreme case of a solid homogeneous panel whereas $\chi/r < 0.1$ is more typical of sandwich panel construction. Since the two curves in figure 3 differ at most by about 6 percent, it is concluded that for the small values of χ/r usually encountered in sandwich panels, the effect of rotary inertia on the modal density is negligible in comparison to the effect of shear flexibility.

The curves given by equation (8) are asymptotic to the curve

$$\frac{1}{(\pi/4)(a/b)} \frac{dN}{d(\omega/\omega_o)} = 2\left(r \frac{\omega}{\omega_o}\right) \tag{9}$$

and for $r(\omega/\omega_o) \geq 3$ this straight line approximates the solid curve of figure 3 to within 1 percent. However, equation (9) implies that the modal density $\Delta N/\Delta\omega$ becomes independent of the face material properties at large values of $r(\omega/\omega_o)$. This physically unrealistic result arises because equation (8) does not account for the bending stiffness of the panel faces.

Effect of face bending stiffness- In view of the results of the previous section it is assumed here that rotary inertia can be neglected. Equation (2) can then be used to determine the effect of face bending stiffness on the modal density. For an isotropic core, equation (2) can be written as

$$r \frac{\omega}{\omega_o} = r\rho^2 \sqrt{\tau + \frac{1}{1 + r\rho^2}} \tag{10}$$

which is independent of θ. Use of equation (5) yields

$$\frac{1}{\frac{\pi}{4}\frac{a}{b}} \frac{dN}{d\left(\frac{\omega}{\omega_o}\right)} \simeq \frac{1}{\frac{\partial(\omega/\omega_o)}{\partial\rho^2}} = \frac{\sqrt{1 + r\rho^2}}{\sqrt{1 + \tau(1 + r\rho^2)}\left\{1 - \frac{r\rho^2}{2(1 + r\rho^2)[1 + \tau(1 + r\rho^2)]}\right\}} \tag{11}$$

for the estimate of modal density. The variation in modal density with $r(\omega/\omega_o)$ is obtained from equations (10) and (11) by treating τ as a parameter and the quantity $r\rho^2$ as a variable. For the case of identical face sheets, this variation is shown in figure 4 for various values of the face to core thickness ratio t_f/h_c. It is seen that neglecting the face bending stiffness ($t_f/h_c = 0$ curve) leads to an overestimate of the modal density by an amount that increases with increasing frequency and with increasing ratios of face to core thickness. However, for many sandwich configurations t_f/h_c is on the order of 0.1 or less and often the quantity r/ω_o is so small that a frequency of several thousand Hertz is required to produce a value of $r(\omega/\omega_o)$ on the order of 1.0. Thus, there are many practical situations where the face bending stiffness can be neglected when computing the modal density.

When the face bending stiffness should be taken into account, the following simple equation is useful

$$\frac{1}{(\pi/4)(a/b)}\frac{dN}{d(\omega/\omega_o)} \simeq \frac{2r(\omega/\omega_o)}{\sqrt{1 + \tau[2r(\omega/\omega_o)]^2}} \tag{12}$$

For $r(\omega/\omega_o) \geq 3$ and $t_f/h_c \leq 0.2$ (identical face sheets), this result predicts modal density values that are within about 1 percent of the values given by the exact solution. (Eq. (12) is obtained from eqs. (10) and (11) by taking $r\rho^2 >> 1$.)

Flat Sandwich Beam

The differential equations in appendix B can be applied to a flat beam whose length b is in the y direction if all terms that involve the x coordinate are dropped. This has the effect of eliminating the thickness-twist solution and all terms involving $m/(a/b)$ from the bending and thickness-shear solutions. Thus, the frequency equation for the beam "bending" modes can be obtained directly from the panel "bending" solution by setting the $m/(a/b)$ terms equal to zero. The modal density is then simply obtained from $dN/d(\omega/\omega_o) \simeq dn/d(\omega/\omega_o)$.

Face bending stiffness neglected- This case is obtained by setting $m/(a/b) = 0$ in equation (7). Differentiating with respect to ω/ω_o yields

$$\frac{dN}{d\left(\frac{\omega}{\omega_o}\right)} \simeq \frac{\left(1 + \frac{\chi}{r}\right)\left(r\,\frac{\omega}{\omega_o}\right) + \frac{2 + \left(1 - \frac{\chi}{r}\right)^2\left(r\,\frac{\omega}{\omega_o}\right)^2}{\sqrt{4 + \left(1 - \frac{\chi}{r}\right)^2\left(r\,\frac{\omega}{\omega_o}\right)^2}}}{\sqrt{2\left(\frac{\omega}{\omega_o}\right)}\sqrt{\left(1 + \frac{\chi}{r}\right)\left(r\,\frac{\omega}{\omega_o}\right) + \sqrt{4 + \left(1 - \frac{\chi}{r}\right)^2\left(r\,\frac{\omega}{\omega_o}\right)^2}}} \tag{13}$$

The variation in modal density with frequency, as given by equation (13), is shown in figure 5 for various values of the shear flexibility parameter r and for two values of χ/r. As in the case of panels, realistic values of χ/r give essentially the same results as $\chi = 0$ (rotary inertia neglected). The $r = \chi = 0$ curve corresponds to classical beam theory, which predicts that modal density decreases with increasing frequency. When shear flexibility is accounted for ($r > 0$), equation (13) predicts that the beam modal density is nearly constant over a wide frequency range. However, this result is valid only for conditions where the face bending stiffness is unimportant.

Effect of face bending stiffness- If rotary inertia is neglected, equation (2) can be used to determine the effect of the face bending stiffness on a beam's modal density by letting $m/(a/b) = 0$. The result is

$$\frac{\omega}{\omega_o} = n^2\sqrt{\tau + \frac{1}{1 + rn^2}} \tag{14}$$

$$\frac{dN}{d\left(\frac{\omega}{\omega_o}\right)} \simeq \frac{1}{\frac{d(\omega/\omega_o)}{dn}} = \frac{\sqrt{1 + rn^2}}{2n\sqrt{1 + \tau(1 + rn^2)}} \left\{ 1 - \frac{rn^2}{2(1 + rn^2)[1 + \tau(1 + rn^2)]} \right\} \quad (15)$$

The variation in modal density with frequency as given by equations (14) and (15) is shown in figure 6 for several values of r and with a face-to-core thickness ratio of 0.05 (identical face sheets). Comparison of the curves in figure 6 with the corresponding curves in figure 5 reveals that neglect of the face bending stiffness again leads to an overestimate of the modal density by an amount that increases with increasing frequency. The face bending stiffness is also seen to have a smaller effect on beams with stiff cores (small r) than on beams with more flexible cores (larger r).

Figures 5 and 6 both indicate a large rise in modal density as ω/ω_o approaches zero. However, it must be remembered that the equations presented for modal density are estimates that have been obtained by representing the number of modes by a continuous function of frequency. Such a representation is not really meaningful at frequencies near that of the fundamental mode $\omega/\omega_o \simeq 1$ as there are usually too few modes involved. This is illustrated in figures 5 and 6 by the line labeled $N \geq 6$. For frequencies to the left of this line only five modes exist. Thus, the large rise in modal density as $\omega/\omega_o \to 0$ is physically unrealistic. A similar situation occurs in the modal density estimates for curved panels.

Curved Sandwich Panel With Isotropic Core

Face bending stiffness neglected- When the parameter C is retained in equation (1), the effects of panel curvature can be determined. For an isotropic core ($r = r_x = r_y$), the "bending set" of modes is described by

$$2\rho^2 = (r + \chi)\left(\frac{\omega}{\omega_o}\right)^2 - rC^2 \cos^4(\theta)$$

$$+ \sqrt{\left[(r - \chi)\left(\frac{\omega}{\omega_o}\right)^2 - rC^2 \cos^4(\theta)\right]^2 + 4\left[\left(\frac{\omega}{\omega_o}\right)^2 - C^2 \cos^4(\theta)\right]} \quad (16)$$

The modal density is then given by

$$\frac{1}{\frac{\pi}{4}\frac{a}{b}} \frac{dN}{d\left(\frac{\omega}{\omega_o}\right)} \simeq \frac{2}{\pi} \left[\left(1 + \frac{\chi}{r}\right)\left(r\,\frac{\omega}{\omega_o}\right)\left(\frac{\pi}{2} - \theta_1\right) + \int_{\theta_1}^{\pi/2} \frac{2 + \left(\alpha - \frac{\chi}{r}\right)\left(1 - \frac{\chi}{r}\right)\left(r\,\frac{\omega}{\omega_o}\right)^2}{\sqrt{4\alpha + \left(\alpha - \frac{\chi}{r}\right)^2\left(r\,\frac{\omega}{\omega_o}\right)^2}}\, d\theta \right] \quad (17)$$

where

$$\alpha = 1 - \left(\frac{C}{\omega/\omega_o}\right)^2 \cos^4(\theta)$$

The lower limit of integration is

$$\theta_1 = \cos^{-1}\left\{\left(\frac{\omega/\omega_o}{C}\right)^2\left(1 - \frac{\chi}{r}\right) + \frac{2}{(rC)^2}\left[1 - \sqrt{1 - \left(r\,\frac{\omega}{\omega_o}\sqrt{\frac{\chi}{r}}\right)^2}\right]\right\}^{1/4}$$

if

$$r\,\frac{\omega}{\omega_o}\sqrt{\frac{\chi}{r}} \leq 1$$

and

$$\left(\frac{\omega/\omega_o}{C}\right)^2\left(1 - \frac{\chi}{r}\right) + \frac{2}{(rC)^2}\left[1 - \sqrt{1 - \left(r\,\frac{\omega}{\omega_o}\sqrt{\frac{\chi}{r}}\right)^2}\right] \leq 1$$

are <u>both</u> satisfied; otherwise $\theta_1 = 0$.

When $\chi = r = 0$ (rotary inertia and shear flexibility neglected), equation (17) can be expressed in terms of the complete elliptic integral of the first kind (ref. 16). For nonzero values of χ and r, equation (17) is expressible as a hyperelliptic integral. Some hyperelliptic integrals can be reduced to the sum of elliptic integrals; however, the results presented herein were obtained by numerically integrating equation (17). These results are presented in figure 7, where the variation in modal density with $(\omega/\omega_o)/C$ is shown for various values of the product rC. The numerical results shown in figure 7 are all for $\chi = 0$ (rotary inertia neglected).[3] However, in view of the relatively insignificant effect of rotary inertia on the modal densities of the beam and flat panel, it is likely that the curves in figure 7 would be only slightly altered by realistic values of χ/r.

The peaks in modal density about $\omega/\omega_o = C$ (the so-called "ring frequency") are due to a concentration of modes occurring near this frequency and is most pronounced for the $r = 0$ case. However, the sharp spike is due to the singularity in equation (17) at $\omega/\omega_o = C$ (when $\chi = 0$) and is physically

[3]For $\chi = 0$ and $(\omega/\omega_o)/C \leq 1$, the integrand of equation (17) diverges at θ_1, but for $(\omega/\omega_o)/C \neq 1$, the integral is convergent. In the numerical integration of equation (17) the contribution of the integrand in the neighborhood of θ_1 was approximated by replacing the integrand with the first three terms of its Taylor series representation. For $r = \chi = 0$, the results obtained in this manner agree within 0.5 percent of the results given by the elliptic integral solution.

unrealistic. A better estimate for the peaks in modal density about the ring frequency can be obtained by directly calculating the number of curved panel modes ΔN_C occurring there from the frequency equation

$$\left(\frac{\omega}{\omega_o}\right)^2 = \frac{\left[\left(\frac{m}{a/b}\right)^2 + n^2\right]^2}{1 + r\left[\left(\frac{m}{a/b}\right)^2 + n^2\right]} + \frac{C^2\left(\frac{m}{a/b}\right)^4}{\left[\left(\frac{m}{a/b}\right)^2 + n^2\right]^2} \tag{18}$$

(Eq. (18) is obtained from eq. (16) or (4).)

For $r = 0$, the results of such calculations for the interval $0.95C < \omega/\omega_o < 1.05C$ are presented in table 1 for various degrees of curvature (a/b was taken equal to $4/\pi$). The number of modes ΔN_F that the corresponding flat panel has in the same frequency interval is also shown for comparison.

TABLE 1.- COMPARISON OF CURVED AND FLAT PANEL MODAL DENSITIES AT THE RING FREQUENCY ($r = X = 0$)

Curvature parameter C	Frequency interval $0.95C < \omega/\omega_o < 1.05C$	Number of modes in frequency interval		$\frac{\Delta N_C}{\Delta N_F}$
		Flat panel ΔN_F	Curved panel ΔN_C	
50	47.5 → 52.5	5	5	1.0
75	71.25 → 78.75	6	8	1.33
100	95 → 105	10	13	1.30
200	190 → 210	21	27	1.29
300	285 → 315	29	43	1.48
400	380 → 420	39	55	1.41
500	475 → 525	49	76	1.55
750	712.5 → 787.5	76	115	1.51
1000	950 → 1050	101	155	1.53

For $300 \leq C \leq 1000$, the actual peak in curved panel modal density is about 1-1/2 times that of the flat panel value. This result is indicated in figure 7. For $75 \leq C < 300$, a somewhat smaller increase is evident. For C less than about 50 the effect of curvature is so small that the panel essentially behaves as if it were flat, not only at $0.95 < (\omega/\omega_o)/C < 1.05$ but over the entire frequency range.

Except in the $r = 0$ case, figure 7 obscures the fact that when ω/ω_o exceeds C the curved panel modal density becomes asymptotic to that of the corresponding flat panel ($C = 0$). This behavior is more clearly seen by replotting figure 7 in terms of $r(\omega/\omega_o)$ for fixed values of rC as shown by the solid curves in figure 8. The curve labeled $rC = 0$ denotes the flat panel solution. Because of the singularity in equation (17), the modal densities at $\omega/\omega_o = C$ were estimated from equation (18) in the same manner as was done for $r = 0$. There is essentially no difference, at or above the ring frequency, between the curved and flat panel results whenever the product rC is greater than two.

Useful approximations to the solid curves in figure 8 are given by the equation

$$\frac{1}{(\pi/4)(a/b)}\frac{dN}{d(\omega/\omega_o)} = \begin{cases} 2r\,\dfrac{\omega}{\omega_o}\,\dfrac{\sin^{-1}\sqrt{r(\omega/\omega_o)/rC}}{\pi/2} & \text{for} \quad \dfrac{\omega/\omega_o}{C} < 1 \\ 2r\,\dfrac{\omega}{\omega_o} & \text{for} \quad \dfrac{\omega/\omega_o}{C} > 1 \end{cases} \tag{19}$$

Results from equation (19) are shown by the dashed curves in figure 8. It is seen that this simple approximation to the solution of equation (17) is fairly accurate for values of rC greater than about 3 if $r(\omega/\omega_o)$ is greater than about $rC/3$. (Eq. (19) is obtained by taking $r\rho^2 >> 1$ and $\chi = 0$ in eq. (16) with $\theta_1 = \cos^{-1}\sqrt{(\omega/\omega_o)/C}$ and $\theta_2 = \pi/2$ in eq. (5).)

Effect of face bending stiffness- Since equation (17) does not account for the face bending stiffness, it undoubtedly overestimates the modal density at the larger values of $r(\omega/\omega_o)$. (The curves in fig. 7 correspond to $0 \le r(\omega/\omega_o) \le 10$.) At the larger values of $r(\omega/\omega_o)$ an approximate solution giving the combined effect of panel curvature and face bending stiffness can be obtained from equation (4) by neglecting 1 with respect to $r\rho^2$ as in the derivation of equations (12) and (19). This leads to

$$\frac{1}{(\pi/4)(a/b)}\frac{dN}{d(\omega/\omega_o)} \simeq \frac{2r(\omega/\omega_o)}{\sqrt{1 + \tau[2r(\omega/\omega_o)]^2}} \int_{\theta_1}^{\pi/2} \frac{d\theta}{(\pi/2)\sqrt{1 - \delta^2\cos^4\theta}} \tag{20a}$$

where

$$\delta^2 = \frac{\tau(2rC)^2}{1 + \tau[2r(\omega/\omega_o)]^2} \tag{20b}$$

and

$$\theta_1 = \begin{cases} 0 & \text{if} \quad \dfrac{\omega/\omega_o}{C} \ge 1 \\ \cos^{-1}\sqrt{\dfrac{\omega/\omega_o}{C}} & \text{if} \quad \dfrac{\omega/\omega_o}{C} < 1 \end{cases} \tag{20c}$$

By making the substitution $t = \cos^2\theta$, equation (20a) takes the form of equation 254.00 of reference 19 and can be expressed as follows.

For $\delta \leq 1$:

$$\left.\begin{aligned} \frac{1}{(\pi/4)(a/b)} \frac{dN}{d(\omega/\omega_o)} &\simeq \frac{2r(\omega/\omega_o)}{\sqrt{1 + \tau[2r(\omega/\omega_o)]^2}} \frac{F(\phi_1,k_1)}{\pi/2} \frac{1}{\sqrt{1+\delta}} \\ \text{where} \quad k_1 &= \sqrt{\frac{2\delta}{1+\delta}} \\ \text{and} \quad \phi_1 &= \begin{cases} \frac{\pi}{2} & \text{if} \quad \frac{\omega/\omega_o}{C} \geq 1 \\ \sin^{-1}\sqrt{\frac{[(\omega/\omega_o)/C](1+\delta)}{1+\delta[(\omega/\omega_o)/C]}} & \text{if} \quad \frac{\omega/\omega_o}{C} < 1 \end{cases} \end{aligned}\right\} \quad (21a)$$

For $\delta \geq 1$:

$$\left.\begin{aligned} \frac{1}{(\pi/4)(a/b)} \frac{dN}{d(\omega/\omega_o)} &\simeq \frac{2r(\omega/\omega_o)}{\sqrt{1 + \tau[2r(\omega/\omega_o)]^2}} \frac{F(\phi_2,k_2)}{\pi/2} \frac{1}{\sqrt{2\delta}} \\ \text{where} \quad k_2 &= \sqrt{\frac{1+\delta}{2\delta}} \\ \text{and} \quad \phi_2 &= \sin^{-1}\sqrt{\frac{2\delta[(\omega/\omega_o)/C]}{1+\delta[(\omega/\omega_o)/C]}} \end{aligned}\right\} \quad (21b)$$

In equations (21a) and (21b), $F(\phi,k)$ is the incomplete elliptic integral of the first kind.

The variation in modal density with $r(\omega/\omega_o)$ as given by equations (21) is shown by the solid curves in figures 9(a) through 9(c) for values of rC equal to 3, 5, and 10, respectively. Each figure is for identical face sheets with a face-to-core thickness ratio of $t_f/h_c = 0.1$.

The exact solution for the modal density based on the entirety of equation (4) has not been obtained. Without having this exact solution, the errors introduced by the approximation $r\rho^2 >> 1$, on which equations (21) are based, cannot be firmly established. However, for $C = 0$ (flat panel) and $\tau = 0$ (face bending stiffness neglected), equations (21) reduce to the approximate solutions given by equations (12) and (19), respectively. The latter two approximate solutions were shown to agree well with the corresponding exact solutions (eqs. (11) and (17), respectively) over certain parameter ranges. This suggests that the solution given by equations (21) may also be a fairly reliable estimate of the modal density for the same range of parameters.

In the case of the flat panel, the effect of the face bending stiffness is relatively small for $r(\omega/\omega_o) < 5$ and $t_f/h_c \leq 0.1$ (see fig. 4). Thus, if the ring frequency is in this range ($rC < 5$), the modal density below the ring frequency would be expected to be significantly affected by the curvature and only slightly affected by the face bending stiffness. The approximate solution given by equations (21) does predict this behavior as can be seen from figures 9(a) and 9(b) ($rC = 3$ and 5, respectively). Below the ring frequency the approximate solution (solid curve) closely follows the exact solution (dot-dashed curve) for the curved panel without face bending stiffness given by equation (17). Above the ring frequency, the approximate solution closely follows the exact flat panel solution (dashed curve) given by equation (11).

Next, consider the ring frequency in the frequency range where the face bending stiffness of the flat panel becomes important ($rC > 5$ for $t_f/h_c = 0.1$). In this situation, the modal density below the ring frequency would be expected to increase at a less rapid rate than given by equation (17). This too is predicted by equations (21) as shown in figure 9(c) ($rC = 10$) by the increased separation between the solid and dot-dashed curves in the range $5 \leq r(\omega/\omega_o) < 10$. Above the ring frequency ($r(\omega/\omega_o) > 10$ in fig. 9(c)), the approximate solution again approaches the exact flat panel solution.

As a further check on the solution given by equations (21) the modal density for $rC = 10$ was determined directly from equation (4) by counting the actual number of modes occurring in intervals of $\Delta[r(\omega/\omega_o)] = 1.0$. The values for the modal density obtained in this manner are shown by the circular symbols in figure 9(c) and are quite close to the estimate (solid curve) given by equations (21). (The parameter values used for this computation were $a/b = 1.27$, $C = 200$, $r = 0.05$, and $t_f/h_c = 0.1$.)

Effect of Core Orthotropy

Face bending stiffness neglected- When the effects of face bending stiffness and rotary inertia are neglected, the equation governing ρ^2 for a curved sandwich panel having an orthotropic core is obtained from equation (1) by setting $\chi = 0$. This yields

$$\left(1 + \frac{1 - \mu}{2}\frac{r_y}{\gamma}\rho^2\right)\left\{\rho^4 - \left[\left(\frac{\omega}{\omega_o}\right)^2 - C^2\cos^4(\theta)\right]\left(1 + r_y\rho^2\right)\right\}$$
$$+ r_y\left(\frac{\gamma - 1}{\gamma}\right)\left\{\frac{1 - \mu}{2}\rho^4 + \left[\left(\frac{\omega}{\omega_o}\right)^2 - C^2\cos^4(\theta)\right]\left(1 - \frac{1 - \mu}{2}\right)\right\}\rho^2\cos^2(\theta) = 0 \quad (22)$$

Except when $\gamma = 1$ (isotropic core), equation (22) is cubic in ρ^2 and no attempt is made to solve it in this form. However, an indication of the effect of γ can be obtained by considering the conditions

$$\frac{r_y\rho^2}{\gamma} >> 1 \qquad r_y\rho^2 >> 1 \quad (23)$$

Under these conditions ρ^2 is approximately equal to

$$\rho^2 \approx \frac{r_y[(\omega/\omega_o)^2 - C^2 \cos^4(\theta)]}{\gamma\{1 - [(\gamma - 1)/\gamma]\sin^2(\theta)\}} > 0 \tag{24}$$

Substituting into equation (5), and noting that $\theta_1 = 0$ and $\theta_2 = \pi/2$, yields

$$\frac{1}{(\pi/4)(a/b)} \frac{dN}{d(\omega/\omega_o)} \approx 2\left(\frac{r_y}{\sqrt{\gamma}}\right)\left(\frac{\omega}{\omega_o}\right) \tag{25}$$

Comparison of this result with equation (9) suggests that the isotropic results can perhaps be applied to panels with orthotropic cores if r is replaced with an effective shear-flexibility parameter $r_{eff} = r_y/\sqrt{\gamma}$. However, it is also likely that C will have to be replaced with an effective curvature parameter since equation (25) is not valid where the effects of curvature are expected to be most pronounced ($\omega/\omega_o \leq C$).[4]

This idea was examined by solving equation (22) for ω/ω_o in terms of m and n:

$$\left(\frac{\omega}{\omega_o}\right)^2 = \frac{\{[m/(a/b)]^2 + n^2\}^2}{1 + \zeta} + \frac{C^2[m/(a/b)]^4}{\{[m/(a/b)]^2 + n^2\}^2} \tag{26}$$

where ζ is the same as in equation (3b).

For specified values of a/b, r_y, γ, μ, and C, the number of modes N existing below any frequency ω/ω_o can be calculated from equation (26) and a plot of N vs. ω/ω_o is readily constructed as shown in figure 10. The possibility of duplicating this plot (hence the modal density) by calculating N from the isotropic frequency equation (eq. (18)) with r replaced by some r_{eff} and with C replaced by some C_{eff} was then considered; that is, from

$$\left(\frac{\omega}{\omega_o}\right)^2 = \frac{\{[m/(a/b)]^2 + n^2\}^2}{1 + r_{eff}\{[m/(a/b)]^2 + n^2\}} + \frac{C_{eff}^2[m/(a/b)]^4}{\{[m/(a/b)]^2 + n^2\}^2} \tag{27}$$

The two curves in figure 10 were obtained from the exact equation (eq. (26)) and show that, for $r_y/\sqrt{\gamma}$ held constant, a decrease in γ (stiffening of core in circumferential direction) causes a decrease in the cumulative number of modes. This same effect is produced by eqaution (27), for r_{eff} held constant, if C_{eff} is made to increase as γ decreases. For

[4]The inequality $\rho^2 > 0$ expressed by equation (24) cannot be satisfied at $\theta = \theta_1$ if $\omega/\omega_o \leq C$.

values of γ from 0.4 to 2.5 (representative of honeycomb cores) with $1 \leq a/b \leq 2.55$, $r_y/\sqrt{\gamma}$ up to 0.125, and C up to 500, it was found that the plots of N vs. ω/ω_o obtained from equation (26) were duplicated quite well by equation (27) if r_{eff} and C_{eff} were taken as

$$r_{eff} = \frac{r_y}{\sqrt{\gamma}} = \frac{\pi^2}{b^2} \frac{D_s}{\sqrt{D_{Q_x} D_{Q_y}}} \tag{28a}$$

$$C_{eff} = \begin{cases} \dfrac{C}{(\gamma)^{0.15}} & \text{if} \quad \dfrac{\omega/\omega_o}{C} \leq 0.9 \\ C & \text{if} \quad \dfrac{\omega/\omega_o}{C} > 0.9 \end{cases} \tag{28b}$$

If the above expressions for r_{eff} and C_{eff} are used, equation (27) (empirical) predicts modal densities that are within 5 percent of the results predicted by equation (26) (exact) for a flat panel and also for a curved panel when $(\omega/\omega_o)/C$ is greater than 0.9. In the range $0.1 \leq (\omega/\omega_o)/C \leq 0.90$, the accuracy of equation (27) depends on $r_{eff}C$. For $r_{eff}C \leq 2$, the average error in the modal density is less than 5 percent; as $r_{eff}C$ increases to 5, the average error increases to about 10 percent, and for $r_{eff}C = 10$, the average error is about 15 percent. Typical results are shown in figures 11(a) and 11(b). Figure 11(a) shows exact plots of N vs. ω/ω_o for $C = 0$ and $C = 100$ with $r_y = 0.00707$, $\gamma = 1/2$, and $a/b = 2.55$. The corresponding plots obtained from equation (27) with r_{eff} and C_{eff} defined by equations (28) are shown in figure 11(b).

The form of equation (27) is exactly the same as equation (18). Thus, when rotary inertia and face bending stiffness effects are small, the modal density estimates obtained for panels having isotropic cores appear applicable to panels having moderately orthotropic cores such as honeycomb by simply replacing r and C with the quantities r_{eff} and C_{eff}, respectively, defined by equations (28). Note that the "effective" shear stiffness is the geometric mean of the two orthotropic stiffnesses.

Another check on the validity of this empirical approach is that for a flat panel, equations (27) and (28) predict the variation in N with ω/ω_o to be unaffected by a 90° core rotation. This has been verified by using equation (26) (the exact equation) to show that, for the range $0.4 \leq \gamma \leq 2.5$, plots of N vs. ω/ω_o are indeed unaffected by such a rotation. A typical example is shown in figures 12(a) and 12(b). Figure 12(a) is for a flat panel ($C = 0$) with $r_y = 0.00707$, $\gamma = 1/2$, and $a/b = 1.27$. Figure 12(b) corresponds to the same flat panel but with the core rotated 90° ($r_y = 0.01414$, $\gamma = 2$). The resulting curves of N vs. ω/ω_o are virtually identical.

Effect of face bending stiffness- In the case of a flat panel an approximate solution giving the combined effect of orthotropic core shear moduli and face bending stiffness on the modal density can be obtained by neglecting certain terms in equation (2). If the conditions given by equations (23) are

satisfied, then by order-of-magnitude considerations, equation (2) simplifies to the approximation

$$r_y \tau \rho^4 + [1 + (\gamma - 1)\cos^2\theta]\rho^2 - r_y\left(\frac{\omega}{\omega_o}\right)^2 \approx 0 \tag{29}$$

Solving for $\partial\rho^2/\partial(\omega/\omega_o)$, substituting into equation (5), and noting that $\theta_1 = 0$ and $\theta_2 = \pi/2$, yields

$$\frac{1}{(\pi/4)(a/b)}\frac{dN}{d(\omega/\omega_o)} \approx \frac{2r_y(\omega/\omega_o)}{\pi/2}\int_o^{\pi/2}\frac{d\theta}{\sqrt{\tau[2r_y(\omega/\omega_o)]^2 + [1 + (\gamma - 1)\cos^2\theta]^2}} \tag{30}$$

Making the substitution $t = -(\gamma - 1)\cos^2\theta$ reduces equation (30) to the form of equation 259.00 of reference 19 so that the solution is

$$\frac{1}{(\pi/4)(a/b)}\frac{dN}{d(\omega/\omega_o)} \approx \left(2r_{eff}\frac{\omega}{\omega_o}\right)\beta^{1/4}\frac{K(k)}{\pi/2} \tag{31}$$

where

$$\left.\begin{aligned} r_{eff} &= \frac{r_y}{\sqrt{\gamma}} = \frac{\pi^2}{b^2}\frac{D_s}{\sqrt{D_{Q_x}D_{Q_y}}} \\ \beta &= \frac{\gamma}{\left[1 + \gamma\tau\left(2r_{eff}\frac{\omega}{\omega_o}\right)^2\right]\left[\gamma + \tau\left(2r_{eff}\frac{\omega}{\omega_o}\right)^2\right]} \\ 2k^2 &= 1 - \left[1 + \tau\left(2r_{eff}\frac{\omega}{\omega_o}\right)^2\right]\sqrt{\beta} \end{aligned}\right\} \tag{32}$$

and $K(k)$ is the complete elliptic integral of the first kind.

The terms in equation (31) that involve the orthotropic shear moduli are β and r_{eff}. Both of these terms, and therefore the modal density given by equation (31), are unaffected by a 90° rotation of the core. This is shown in figure 13 by the dashed curves labeled $\gamma = 1/2$ or 2, $\gamma = 1/4$ or 4, and $\gamma = 1/8$ or 8. The solid curve is for an isotropic core ($\gamma = 1$) and is obtained from the exact solution (eq. (11)). All the curves shown in figure 13 are for identical faces with a face-to-core thickness ratio of $t_f/h_c = 0.1$.

Note that equation (31) depends on both $\sqrt{D_{Q_x}D_{Q_y}}$ and $\gamma = D_{Q_x}/D_{Q_y}$. It is only when the face bending stiffness is negligible that the effect of an orthotropic core on the modal density of a flat panel can be described solely in terms of the effective shear stiffness $D_{Q_{eff}} = \sqrt{D_{Q_x}D_{Q_y}}$.

For $\gamma = 1$ (isotropic core), equation (31) reduces to equation (12). This suggests that for the moderately small range of γ usually encountered in honeycomb cores ($0.4 < \gamma < 2.5$), equation (31) should be fairly accurate if $t_f/h_c \leq 0.2$ and $r_{eff}(\omega/\omega_o) \geq 3$ are both satisfied.

EXPERIMENT

Few experimental data are available in the literature on the mode shapes and natural frequencies of vibrating sandwich panels, especially for frequencies substantially above that of the fundamental mode. Although about 35 modes were excited in each of the two panels tested in reference 12, the panel configurations and frequency range were such that the maximum value obtained for $r_{eff}(\omega/\omega_o)$ was about 0.25. At this small value of $r_{eff}(\omega/\omega_o)$, the shear flexibility of the core theoretically has a relatively small effect on the modal density (see fig. 3). Thus, it was necessary to conduct some experiments that would cover a higher range in $r_{eff}(\omega/\omega_o)$ for the purpose of obtaining results that could be compared with theory.

Apparatus

Sandwich panels- The specimens tested consisted of four flat, rectangular sandwich panels constructed from aluminum honeycomb cores bonded to stainless steel face sheets with a structural adhesive. The effective length and width of each panel (measured between the boundaries of the panel support fixture) were $a = 28.5$ in. (72.4 cm) and $b = 24.0$ in. (61.0 cm), respectively. Table 2 lists the pertinent core and face properties along with the resulting panel parameters. The weight of the bonding material was lumped with the weight of the faces to produce an effective face density called $(\rho_f)_{eff}$.

Values of the core shear moduli were calculated from the following equations (ref. 20)

$$\left.\begin{aligned} G_{L_F} &= \frac{G_s}{\rho_s}\rho_c \frac{[1 + (u/v)\cos\eta]^2}{[1 + (u/v)]^2} \\ G_{L_D} &= \frac{G_s}{\rho_s}\rho_c \frac{1 + (u/v)\cos^2\eta}{1 + (u/v)} \\ G_T &= \frac{G_s}{\rho_s}\rho_c \frac{(u/v)\sin^2\eta}{1 + (u/v)} \end{aligned}\right\} \quad (33)$$

The quantities $G_s = 3.85\times10^6$ lb/in.^{2} (26.5 GN/m^2) and $\rho_s = 2.50\times10^{-4}$ lb-sec^2/in.^{4} (2.67 Mg/m^3) are the shear modulus and density of the honeycomb

TABLE 2.- DESCRIPTION OF TEST PANELS

Length: a = 28.5 in. (72.4 cm), each panel
Width: b = 24.0 in. (61.0 cm), each panel

Materials

Panels 1 and 2: Faces of 302 stainless steel sheet
Cores of 1/8-5052 - 0.002 aluminum honeycomb

Panels 3 and 4: Faces of 321 stainless steel sheet
Cores of 0X-3/16-5052 - 0.0007P overexpanded aluminum honeycomb

Panel	Core properties								Face properties						
	ρ_c		G_{cx}		G_{cy}		h_c		$(\rho_f)_{eff}$		E_f		μ	t_f	
	$\frac{lbf\text{-}sec^2}{in.^4}$	kg/m^3	$lbf/in.^2$	MN/m^2	$lbf/in.^2$	MN/m^2	in.	cm	$\frac{lbf\text{-}sec^2}{in.^4}$	Mg/m^3	$lbf/in.^2$	TN/m^2		in.	mm
1	1.21×10^{-5}	129	131×10^3	903	53.0×10^3	365	0.502	1.28	80.3×10^{-5}	8.58	26×10^6	0.18	0.245	0.0154	0.391
2	1.21×10^{-5}	129	53.0×10^3	365	131×10^3	903	0.502	1.28	81.4×10^{-5}	8.70	26×10^6	0.18	0.245	0.0154	0.391
3	0.316×10^{-5}	33.8	21.7×10^3	150	23.9×10^3	165	0.503	1.28	80.3×10^{-5}	8.58	28×10^6	0.19	0.245	0.0203	0.516
4	0.316×10^{-5}	33.8	23.9×10^3	165	21.7×10^3	150	0.503	1.28	81.1×10^{-5}	8.67	28×10^6	0.19	0.245	0.0203	0.516

Panel	Panel parameters					
	a/b	t_f/h_c	ω_o, rad/sec	r_{eff}	X/r_{eff}	Y
1	1.19	0.0307	738	0.0221	0.0449	2.47
2	1.19	0.0307	734	0.0221	0.0450	0.405
3	1.19	0.0404	843	0.114	0.00993	0.908
4	1.19	0.0404	840	0.114	0.00993	1.10

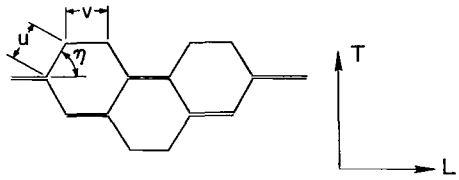

Sketch (a) Geometry of honeycomb cells.

material, respectively; u, v, and η are defined in sketch (a). The honeycomb shear modulus in the longitudinal (L) direction of the core is designated G_L and the shear modulus in the transverse (T) direction of the core is designated G_T. The first and second of equations (33) are lower and upper bounds, respectively, to the longitudinal modulus and the arithmetic average of these values was used for G_L.

Experimental values of shear moduli obtained from single-block shear tests of the overexpanded cores used in panels 3 and 4 were supplied by the honeycomb manufacturer. However, these tests showed considerable scatter with values of $\sqrt{G_L G_T}$ from 21 to 31 percent lower than the result obtained from equations (33). Since values of shear moduli obtained from block shear tests are known to be generally low in comparison with values obtained from theory and other test methods (ref. 21), it is felt that the theoretical values used herein are more accurate than the experimentally obtained values. For the normally expanded cores used in panels 1 and 2, the handbook value of $\sqrt{G_L G_T}$ was within 2 percent of the theoretical result used.

For the cores used in panels 1 and 2, $\eta \approx 43°$ and $u/v \approx 1.6$. For the cores used in panels 3 and 4, $\eta \approx 72°$ and $u/v \approx 1.2$. The approximate geometry of the honeycomb cores and the orientation with respect to each panel is shown in figure 14. Panels 1 and 2 were nearly identical except for a 90° rotation of the core. The primary difference between panels 3 and 4 was also a 90° core rotation.

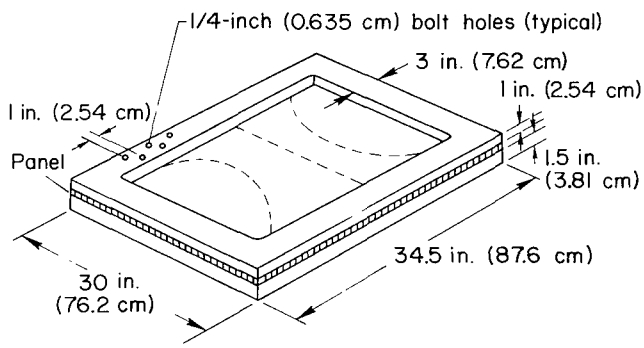

Sketch (b) Panel mounting fixture.

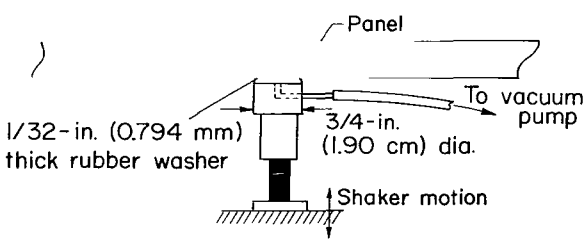

Sketch (c) Vacuum cup attachment.

Support and excitation system- The panel mounting fixture consisted of two aluminum frames bolted to the outer 3 in. (7.62 cm) of the panel perimeter to provide a partially clamped edge condition (see sketch (b)). Each steel bolt was torqued to 175 in.-lb (19.8 m-N). To prevent crushing of the core, the outer 3 in. (7.62 cm) of honeycomb cells were filled with a liquid aluminum potting material.

The fixture was supported by a wooden frame, and the panel was excited from below by a small (25-lb force (111 N)) permanent magnet shaker. The shaker was coupled to the panel surface by means of a small vacuum cup to avoid the fastening of attachment points to the panel (see sketch (c)). This arrangement proved

to be quite satisfactory for transmitting motion to the panel and it allowed the excitation point to be easily changed.

Instrumentation- The shaker was driven by the amplified signal of a variable frequency oscillator. A hand-held vibration pickup was used to detect the panel motion. The frequencies of the oscillator and vibration pickup signals were measured by an electronic frequency counter. These signals were also monitored on an oscilloscope in the form of Lissajous figures.

Test Procedure

For each panel, between 70 and 80 consecutive modes of vibration were excited by varying the frequency and location of the applied excitation. The mode shape at each resonance was visualized by the formation of Chladni figures produced by the collection of sand particles (16 mesh size) along node lines. A few of these sand patterns are shown in figure 15. For some of the higher frequency resonances, the Chladni figures were not sharply defined. In these cases, the phase differences between the oscillator signal and the vibration pickup signals were used to detect the node lines. In some instances, two or more modes occurred at nearly the same frequency, and careful positioning of the excitation point was required to produce distinct Chladni figures.

Test Results

Frequencies are given in table 3 for the four test panels corresponding to the maximum resonance response for the modes listed. The mode number m in the x direction (n in the y direction) indicates $m - 1$ ($n - 1$) lines of zero deflection between the panel boundaries $x = 0$ ($y = 0$) and $x = a$ ($y = b$). For panels 1 and 2 the ratio G_L/G_T was equal to about 2.5, which caused corresponding higher modes of these two panels to occur at significantly difference frequencies. For panels 3 and 4, G_L/G_T was nearly unity, and corresponding modes for these panels occurred at nearly the same frequency.

COMPARISON OF THEORY AND EXPERIMENT

The experimental values of $\{1/[(\pi/4)(a/b)]\}[\Delta N/\Delta(\omega/\omega_o)]$ and their variation with $r_{eff}(\omega/\omega_o)$ are shown in figures 16(a) and 16(b) for panels 1 and 2, respectively, and in figures 16(c) and 16(d) for panels 3 and 4, respectively. The horizontal lines indicate the intervals of $r_{eff}(\omega/\omega_o)$ used to compute the corresponding data points. The solid curve in each figure is the theoretical estimate for modal density given by equation (8) with r replaced by r_{eff}. For all four panels, the quantity χ/r_{eff} is much less than one; therefore, theoretically, the effect of rotary inertia is negligible. For the range of $r_{eff}(\omega/\omega_o)$ and t_f/h_c covered by the experiments, the theoretical effect of the face bending stiffness is also negligible.

TABLE 3.- EXPERIMENTAL RESONANCE FREQUENCIES, H_z

[Panels 1 and 2 heavy line encloses modes for which $r_{eff}(\omega/\omega_o) < 1.1$; panels 3 and 4, $r_{eff}(\omega/\omega_o) < 3.0$]

	m/n	1	2	3	4	5	6	7	8	9	10	11
Panel 1	1	294	713	1130	1890	2470	3070	3720	4360	5020	5660	6330
	2	615	950	1425	1960	2590	3230	3850	4460	5140	5770	
	3	1018	1360	1750	2280	2780	3390	3950	4610	5280	5910	
	4	1600	1840	2200	2620	3180	3790	4310	4920	5520		
	5	2162	2460	2815	3130	3630	4130	4750	5300	5900		
	6	2980	3170	3440	3750	4200	4720	5220	5740			
	7	3716	3870	4010	4370	4780	5230	5750	6220			
	8	4470	4660	4930	5090	5460	5890					
	9	5260	5430	5630	5820	6160						
	10	6070										
Panel 2	1	300	726	1180	2260	3060	3960	4900	5940			
	2	530	991	1560	2350	3170	3990	4970				
	3	940	1300	1780	2450	3270	4120	5080				
	4	1340	1690	2120	2700	3530	4360	5150				
	5	1870	2020	2520	3080	3790	4570	5370				
	6	2290	2510	2890	3440	4090	4820	5630				
	7	2750	2930	3360	3840	4470	5150	5980				
	8	3220	3420	3800	4250	4800	5540					
	9	3710	3960	4240	4610	5220	5870					
	10	4200	4421	4680	5170	5630						
	11	4610	4910	5070	5640	6070						
	12	5130	5360	5590	6080							
	13	5700	5800	6100								
Panel 3	1	280	674	940	1360	1760	2140	2520	2910	3290	3640	
	2	443	760	1070	1430	1810	2200	2630	3020	3360		
	3	810	990	1300	1570	1930	2310	2700	3080	3430		
	4	1010	1230	1500	1770	2110	2440	2800	3140	3500		
	5	1330	1530	1750	1980	2310	2580	2930	3280			
	6	1760	1830	2020	2220	2500	2780	3130	3440			
	7	2000	2140	2290	2490	2700	3000	3350				
	8	2360	2440	2560	2750	2960	3210	3540				
	9	2650	2710	2890	3060	3230	3540					
	10	2950	3050	3200	3300	3500						
	11	3300	3390	3460								
	12	3590										
Panel 4	1	288	638	951	1380	1780	2140	2540	2910	3310	3670	
	2	437	754	1060	1430	1820	2200	2620	3060	3380		
	3	784	990	1260	1580	1940	2300	2700	3100	3460		
	4	981	1220	1480	1780	2100	2450	2800	3130	3590		
	5	1310	1540	1720	2010	2310	2630	2940	3310			
	6	1780	1820	2000	2230	2530	2810	3140	3480			
	7	2030	2130	2290	2490	2720	3010	3360				
	8	2340	2430	2580	2760	2970	3240	3530				
	9	2630	2700	2870	3030	3260	3500					
	10	2930	3050	3210	3340	3540	3730					
	11	3270	3390	3460	3620							
	12	3650	3700									

Comparison of the results presented in figure 16 indicates that the theory gives a fairly good estimate of the average modal density except at the smaller values of $r_{eff}(\omega/\omega_0)$. The values of $r_{eff}(\omega/\omega_0)$ at which the comparison becomes poor correspond to the frequency range in the vicinity of the fundamental mode where relatively few modes occur. In this frequency range, the continuous frequency representation of a discrete number of modes is unrealistic. For example, the first two test points in figure 16(c) represent a total of only five modes. In contrast, the last test point in figure 16(c) represents a total of 24 modes. (Note that this is six times the number of modes predicted by classical plate theory.)

Panels 3 and 4 are nominally identical, the major difference being about a 20 percent variation in γ. However, comparison of figures 16(c) and 16(d) shows that the experimental results obtained from panel 3 fall very close to the theoretical curve at nearly every point while the results from panel 4 are more scattered. This is due to a "clumping" of more than the average number of modes (as predicted by theory) in one frequency interval while an adjacent frequency interval has fewer than the average number of modes. (This clumping effect is also seen in figs. 12(a) and 12(b), for example, at $170 < \omega/\omega_0 < 180$.) Depending on the size of frequency interval chosen, this clumping may or may not produce noticeable variations in modal density from the average. The theory gives only the average modal density and does not predict variations from this average.

It should also be noted that the test panels were fastened in a semi-clamped configuration while the theory was based on simple support boundary conditions. The fairly good agreement between the experimental and theoretical results lends support to the implicit assumption that the modal density of sandwich panels, like single-layered panels, is relatively independent of the boundary conditions.

CONCLUSIONS

Theoretical estimates were obtained for the modal densities of sandwich beams and flat or cylindrically curved sandwich panels. The relative importance of transverse shear flexibility and orthotropic shear moduli of the core, bending stiffness of the faces, rotary inertia, and panel curvature as they affect modal density was evaluated. Experimental values of modal density were obtained from resonance tests of flat rectangular panels having orthotropic cores. From the results of the investigation the following conclusions are noted:

1. Failure to account for the transverse shear flexibility of the core can lead to a significant underestimation of the modal density.

2. The effect of rotary inertia is generally negligible compared to the effect of transverse shear flexibility.

3. For many practical sandwich configurations and frequency ranges, the effect of the face bending stiffness can be neglected.

4. For flat rectangular panels having orthotropic cores, a 90° rotation of the core material with respect to the faces has no effect on the average modal density.

5. Where face bending effects are small, the results obtained for flat and cylindrically curved sandwich panels having isotropic cores can be applied to panels having moderately orthotropic cores, such as honeycomb, by introducing an effective shear modulus and an effective curvature parameter. The effective shear modulus is simply the geometric mean of the two-face parallel shear moduli.

6. The agreement between modal densities predicted by theory and modal densities determined from experiment was generally good except at frequencies near that of the fundamental mode where the theory is not applicable.

Ames Research Center
National Aeronautics and Space Administration
Moffett Field, Calif., 94035, Dec. 2, 1969

APPENDIX A

PANEL STIFFNESS AND INERTIAL PROPERTIES

	Nonidentical faces	Identical faces
D_{f_1}, D_{f_2}	$\frac{E_{f_1} t_{f_1}^3}{12(1-\mu^2)}$, $\frac{E_{f_2} t_{f_2}^3}{12(1-\mu^2)}$	$\frac{E_f t_f^3}{12(1-\mu^2)}$
D_s	$\frac{\left(E_{f_1} t_{f_1}\right)\left(E_{f_2} t_{f_2}\right)}{E_{f_1} t_{f_1} + E_{f_2} t_{f_2}} \frac{h_c^2\left(1 + \frac{t_{f_1} + t_{f_2}}{2h_c}\right)^2}{1-\mu^2}$	$\frac{E_f t_f h_c^2\left(1 + \frac{t_f}{h_c}\right)^2}{2(1-\mu^2)}$
D_{Q_x}, D_{Q_y}	$G_{c_x} h_c\left(1 + \frac{t_{f_1} + t_{f_2}}{2h_c}\right)^2$, $G_{c_y} h_c\left(1 + \frac{t_{f_1} + t_{f_2}}{2h_c}\right)^2$	$G_{c_x} h_c\left(1 + \frac{t_f}{h_c}\right)^2$, $G_{c_y} h_c\left(1 + \frac{t_f}{h_c}\right)^2$
E'	$E_{f_1} t_{f_1} + E_{f_2} t_{f_2}$	$2E_f t_f$
I	$* \rho_{f_1} t_{f_1}\left(d_1^2 + \frac{t_{f_1}^2}{12}\right) + \rho_{f_2} t_{f_2}\left(d_2^2 + \frac{t_{f_2}^2}{12}\right) + \rho_c h_c\left(e^2 + \frac{h_c^2}{12}\right)$	$\frac{\rho_f h_c^3}{12}\left[\frac{\rho_c}{\rho_f} + 6\left(\frac{t_f}{h_c}\right) + 12\left(\frac{t_f}{h_c}\right)^2 + 8\left(\frac{t_f}{h_c}\right)^3\right]$
M	$\rho_c h_c + \rho_{f_1} t_{f_1} + \rho_{f_2} t_{f_2}$	$\rho_c h_c + 2\rho_f t_f$

*d_1, d_2, and e are given in symbols list and were obtained from equation (18) of reference 22.

APPENDIX B

DERIVATION OF EQUATION (1)

The differential equations governing the panel vibrations are obtained from the small deflection theory of reference 11 by adding transverse and rotary inertia terms.

$$\left.\begin{aligned}
&\frac{\partial Q_x}{\partial x} + \frac{\partial Q_y}{\partial y} - \frac{E'}{R^2}\nabla^{-4}\frac{\partial^4 w}{\partial x^4} - M\frac{\partial^2 w}{\partial t^2} = 0 \\
&-\frac{\partial^3 w}{\partial x\,\partial y^2} - \frac{\partial^3 w}{\partial x^3} - \frac{Q_x}{D_s} + \frac{1}{D_{Q_x}}\left(\frac{\partial^2 Q_x}{\partial x^2} + \frac{1-\mu}{2}\frac{\partial^2 Q_x}{\partial y^2}\right) \\
&\qquad + \frac{1}{D_{Q_y}}\frac{1+\mu}{2}\frac{\partial^2 Q_y}{\partial x\,\partial y} + \frac{I}{D_s}\frac{\partial^2}{\partial t^2}\left(\frac{\partial w}{\partial x} - \frac{Q_x}{D_{Q_x}}\right) = 0 \\
&-\frac{\partial^3 w}{\partial x^2\,\partial y} - \frac{\partial^3 w}{\partial y^3} - \frac{Q_y}{D_s} + \frac{1}{D_{Q_y}}\left(\frac{\partial^2 Q_y}{\partial y^2} + \frac{1-\mu}{2}\frac{\partial^2 Q_y}{\partial x^2}\right) \\
&\qquad + \frac{1}{D_{Q_x}}\frac{1+\mu}{2}\frac{\partial^2 Q_x}{\partial x\,\partial y} + \frac{I}{D_s}\frac{\partial^2}{\partial t^2}\left(\frac{\partial w}{\partial y} - \frac{Q_y}{D_{Q_y}}\right) = 0
\end{aligned}\right\} \quad \text{(B1)}$$

In equations (B1), x and y specify the coordinates of a point in the panel's middle surface (fig. 1) and t denotes time. The operator ∇^{-4} is defined by $\nabla^{-4}(\nabla^4 w) = \nabla^4(\nabla^{-4} w) = w$ where $\nabla^4 = \partial^4/\partial x^4 + 2\partial^4/\partial x^2\,\partial y^2 + \partial^4/\partial y^4$.

The motion described by these equations is that a straight line perpendicular to the undeformed middle surface ($z = 0$) remains straight and of constant length after deformation but not necessarily perpendicular to the deformed middle surface. This inclination in the x (or y) direction from a right angle is the average shear angle Q_x/D_{Q_x} (or Q_y/D_{Q_y}) produced by the resultant transverse shear force Q_x (or Q_y) per unit width.

For simply supported edges parallel to the x axis at which the support is applied over the entire thickness, the boundary conditions are (ref. 23)

$$w = M_y = \frac{Q_x}{D_{Q_x}} = 0 \quad \text{(B2)}$$

where the moment M_y (acting about the x axis) is given by

$$M_y = -D_s\left[\frac{\partial^2 w}{\partial y^2} - \frac{1}{D_{Q_y}}\frac{\partial Q_y}{\partial y} + \mu\left(\frac{\partial^2 w}{\partial x^2} - \frac{1}{D_{Q_x}}\frac{\partial Q_x}{\partial x}\right)\right] \tag{B3}$$

The boundary conditions along the edges parallel to the y axis are obtained by interchanging y and x.

Expressions for the lateral deflection and shear angles that satisfy the boundary conditions are

$$\left.\begin{aligned} w(x,y,t) &= A' \sin\frac{m\pi x}{a}\sin\frac{n\pi y}{b}\, e^{i\omega t} \\ \frac{Q_x}{D_{Q_x}}(x,y,t) &= \frac{B'}{D_{Q_x}}\cos\frac{m\pi x}{a}\sin\frac{n\pi y}{b}\, e^{i\omega t} \\ \frac{Q_y}{D_{Q_y}}(x,y,t) &= \frac{C'}{D_{Q_y}}\sin\frac{m\pi x}{a}\cos\frac{n\pi y}{b}\, e^{i\omega t} \end{aligned}\right\} \tag{B4}$$

where m and n are integers designating the number of sinusoidal halfwaves in the x and y directions, respectively, and ω is the panel frequency (rad/sec).

The differential equations (B1) are also satisfied by the above forms for w, Q_x/D_{Q_x}, and Q_y/D_{Q_y} provided that

$$\begin{vmatrix} \left(\frac{C}{\rho^2}\right)^2\left(\frac{m}{a/b}\right)^4 - \left(\frac{\omega}{\omega_o}\right)^2 & \frac{m}{a/b} & n \\ \left(\frac{m}{a/b}\right)\left[\rho^2 - \chi\left(\frac{\omega}{\omega_o}\right)^2\right] & -\left\{1 + r_x\left[\left(\frac{m}{a/b}\right)^2 + \left(\frac{1-\mu}{2}\right)n^2 - \chi\left(\frac{\omega}{\omega_o}\right)^2\right]\right\} & -\left(\frac{1+\mu}{2}\right)\left(\frac{m}{a/b}\right)nr_y \\ n\left[\rho^2 - \chi\left(\frac{\omega}{\omega_o}\right)^2\right] & -\left(\frac{1+\mu}{2}\right)\left(\frac{m}{a/b}\right)nr_x & -\left\{1 + r_y\left[n^2 + \left(\frac{1-\mu}{2}\right)\left(\frac{m}{a/b}\right)^2 - \chi\left(\frac{\omega}{\omega_o}\right)^2\right]\right\} \end{vmatrix} = 0 \tag{B5}$$

Expanding the determinant yields equation (1).

APPENDIX C

CONVERSION OF U.S. CUSTOMARY UNITS TO SI UNITS

The International Systems of Units (SI) was adopted by the Eleventh General Conference on Weights and Measures, Paris, October 1960, in Resolution No. 12 (ref. 24). Conversion factors for the units used herein are given in the following table:

Physical quantity	U.S. customary unit	Conversion factor (*)	SI Unit
Length	in.	0.0254	Meters (m)
Force	lbf	4.448	Newtons (N)
Moment	in.-lbf	0.113	Meter-Newtons (m-N)
Density	$\frac{\text{lbf-sec}^2}{\text{in.}^4}$	1.069×10^7	Kilograms per cubic meter (kg/m^3)
Modulus	$\frac{\text{lbf}}{\text{in.}^2}$	6.895×10^3	Newtons per square meter (N/m^2)

*Multiply value given in U.S. Customary Unit by conversion factor to obtain equivalent value in SI unit.

Prefixes to indicate multiple of units are as follows:

Prefix		Multiple
tera	(T)	10^{12}
giga	(G)	10^9
mega	(M)	10^6
kilo	(k)	10^3
centi	(c)	10^{-2}
milli	(m)	10^{-3}

REFERENCES

1. Dyer, Ira: Statistical Vibration Analysis. International Science and Technology, no. 20, Aug. 1963, pp. 35-41; Discussion, pp. 85-86.

2. Smith, Preston W., Jr.; and Lyon, Richard H.: Sound and Structural Vibration. NASA CR-160, 1965.

3. Dyer, Ira: Response of Space Vehicle Structures to Rocket Engine Noise. Vol. II of Random Vibrations, ch. 7, Stephen H. Crandall, ed., MIT Press, 1963, pp. 177-194.

4. Franken, Peter A.; and Lyon, Richard H.: Estimation of Sound-Induced Vibrations by Energy Methods, With Applications to the Titan Missile. Shock and Vibration Bulletin, Bull. 31, pt. 3, U.S. Dept. of Defense, April 1963, pp. 12-26.

5. Manning, Jerome E.; Lyon, Richard H.; and Scharton, Terry D.: Transmission of Sound and Vibration to a Shroud-Enclosed Spacecraft. Report no. 1431 (Contract no. NAS 5-9601), Bolt Beranek and Newman Inc., Oct. 1966.

6. Scharton, Terry D.; and Yang, Thomas M.: Statistical Energy Analysis of Vibration Transmission Into an Instrument Package. Preprint 670876, SAE, Oct. 1967.

7. Crocker, M. J.; and Price, A. J.: Sound Transmission Using Statistical Energy Analysis. J. Sound Vib., vol. 9, no. 3, May 1969, pp. 469-486.

8. Ungar, Eric E.: Fundamentals of Statistical Energy Analysis of Vibrating Systems. Rep. 1350 (AFFDL-TR-66-52), Bolt Beranek and Newman Inc., May 1966.

9. Wilkinson, J. P. D.: Modal Densities of Certain Shallow Structural Elements. J. Acoust. Soc. Am., vol. 43, no. 2, Feb. 1968, pp. 245-251.

10. Fulton, Robert E.: Effect of Face-Sheet Stiffness on Buckling of Curved Plates and Cylindrical Shells of Sandwich Construction in Axial Compression. NACA TN D-2786, 1965.

11. Stein, Manuel; and Mayers, J.: A Small-Deflection Theory for Curved Sandwich Plates. NACA Rep. 1008, 1951. (Supersedes NACA TN 2017)

12. Raville, M. E.; and Ueng, C. E. S.: Determination of Natural Frequencies of Vibration of a Sandwich Plate. Vol. XXIV, no. 2, of Experimental Stress Analysis, B. E. Rossi, ed., Soc. for Experimental Stress Analysis, 1967, pp. 490-493.

13. Maidanik, Gideon: Response of Ribbed Panels to Reverberant Acoustic Fields. J. Acoust. Soc. Am., vol. 34, no. 6, June 1962, pp. 809-826.

14. Heckl, Manfred: Vibrations of Point Driven Cylindrical Shells. J. Acoust. Soc. Am., vol. 34, no. 10, Oct. 1962, pp. 1553-1557.

15. Millar, David K.; and Hart, Franklin D.: Modal Densities of Thin Circular Cylinders. NASA CR-897, 1967.

16. Bolotin, V. V.: On the Density of the Distribution of Natural Frequencies of Thin Elastic Shells. J. Appl. Math. and Mech., vol. 27, no. 2, Oct. 1963, pp. 538-543.

17. Courant, R.; and Hilbert, D.: Methods of Mathematical Physics. Vol. I, ch. VI, Interscience Publishers Inc., 1953.

18. Mindlin, R. D.; Schacknow, A.; and Deresiewicz, H.: Flexural Vibrations of Rectangular Plates. J. Appl. Mech., vol. 23, no. 3, Sept. 1956, pp. 430-436.

19. Byrd, Paul F.; and Friedman, Morris D.: Handbook of Elliptic Integrals for Engineers and Physicists. Springer-Verlag, 1954.

20. Kelsey, S.; Gellatly, R. A.; and Clark, B. W.: The Shear Modulus of Foil Honeycomb Cores. Aircraft Engineering, Oct. 1958, pp. 294-302.

21. Grayley, M. E.: Shear Stiffness of Sandwich Panels - A Review of Test Methods. J. Roy. Aero. Soc., vol. 70, no. 670, Oct. 1966, pp. 950-951.

22. Fulton, Robert E.: Nonlinear Equations for a Shallow Unsymmetrical Sandwich Shell of Double Curvature. Developments in Mechanics, vol. 1, J. E. Lay and L. E. Malvern, eds., Plenum Press, 1961, pp. 365-380.

23. Libove, Charles; and Batdorf, S. B.: A General Small-Deflection Theory for Flat Sandwich Plates. NACA Rep. 899, 1948. (Supersedes NACA TN 1526)

24. Mechtly, E. A.: The International System of Units - Physical Constants and Conversion Factors. NASA SP-7012, 1964.

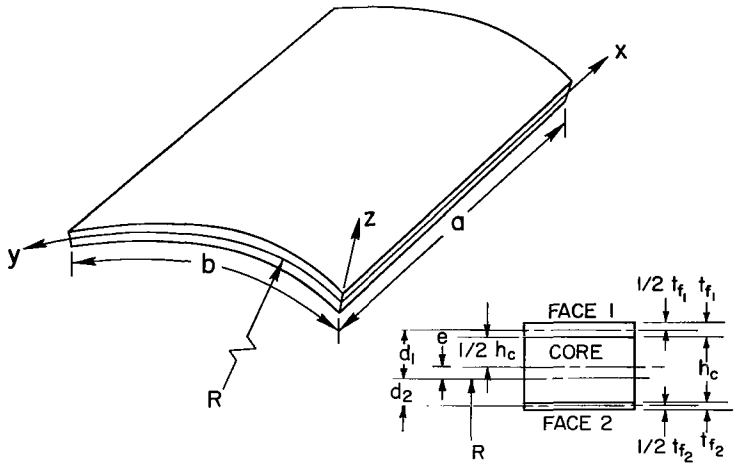

Figure 1.- Panel geometry and coordinate system.

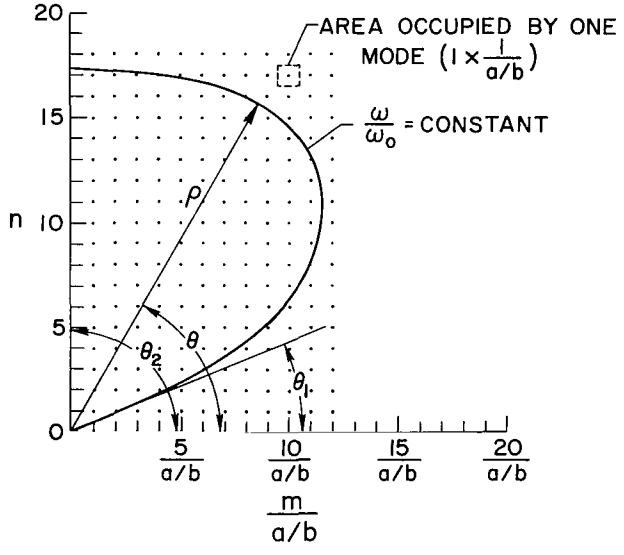

Figure 2.- Modes bounded by a constant frequency curve.

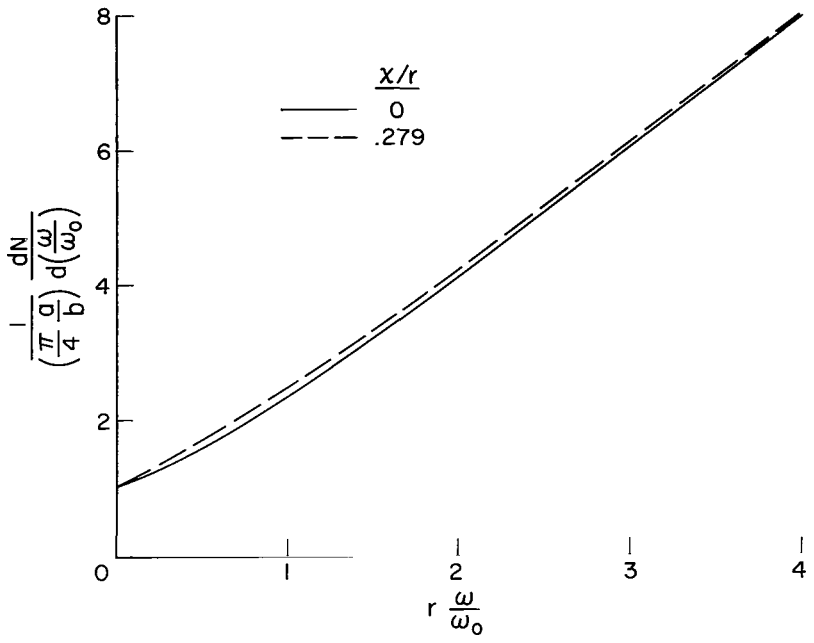

Figure 3.- Effect of shear flexibility and rotary inertia on the modal density of a flat sandwich panel; isotropic core; face bending stiffness neglected.

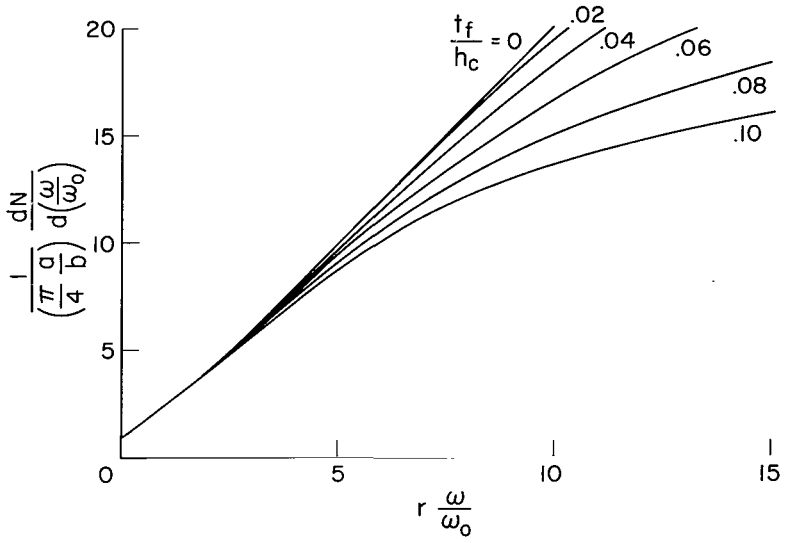

Figure 4.- Effect of shear flexibility and face bending stiffness on the modal density of a flat sandwich panel; isotropic core; rotary inertia neglected.

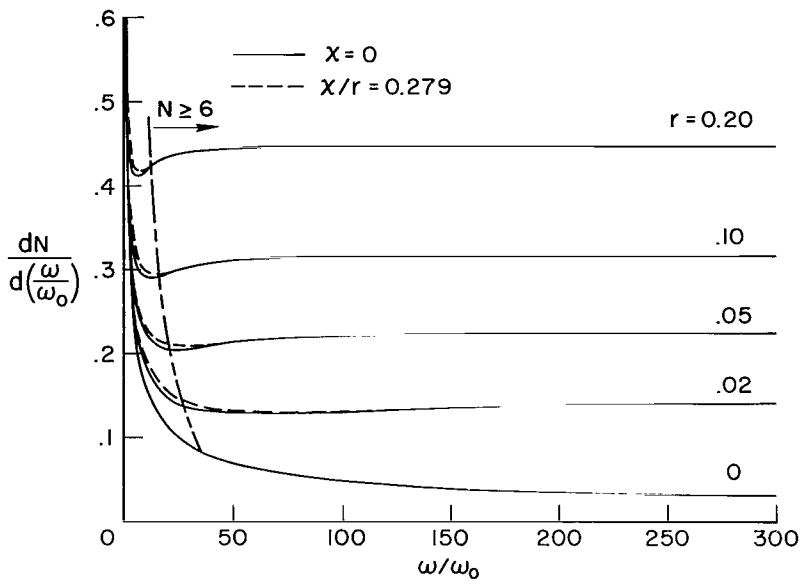

Figure 5.- Effect of shear flexibility and rotary inertia on the modal density of a sandwich beam; face bending stiffness neglected.

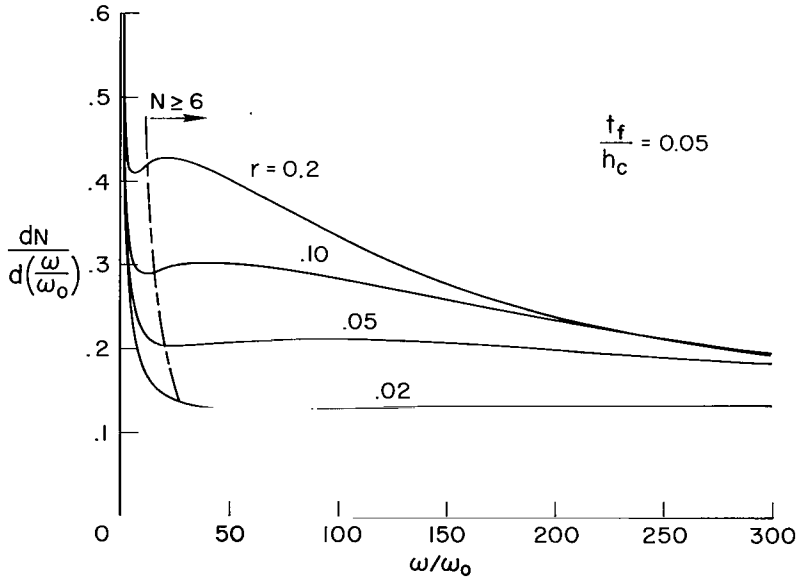

Figure 6.- Effect of shear flexibility and face bending stiffness on the modal density of a sandwich beam; rotary inertia neglected.

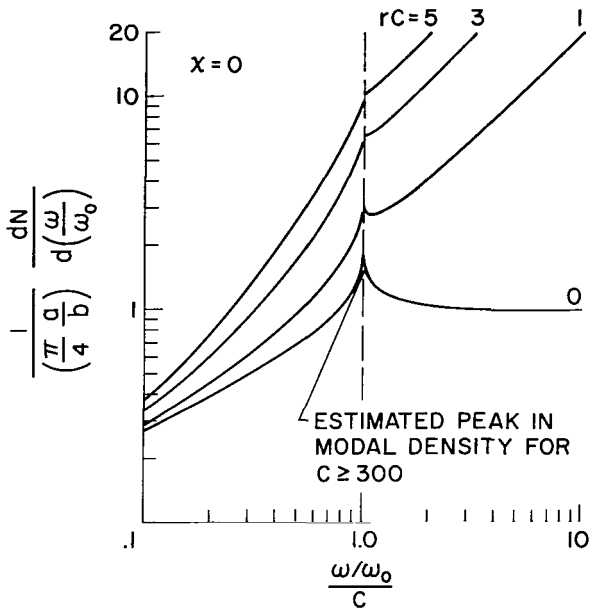

Figure 7.- Modal densities of cylindrically curved sandwich panels; isotropic core; face bending stiffness neglected.

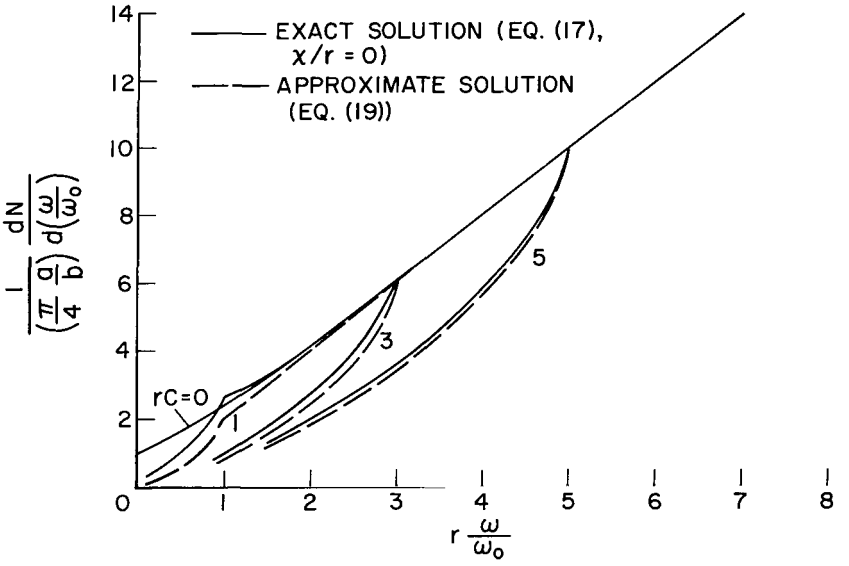

Figure 8.- Asymptotic behavior of cylindrically curved sandwich panel modal density; isotropic core; face bending stiffness and rotary inertia neglected.

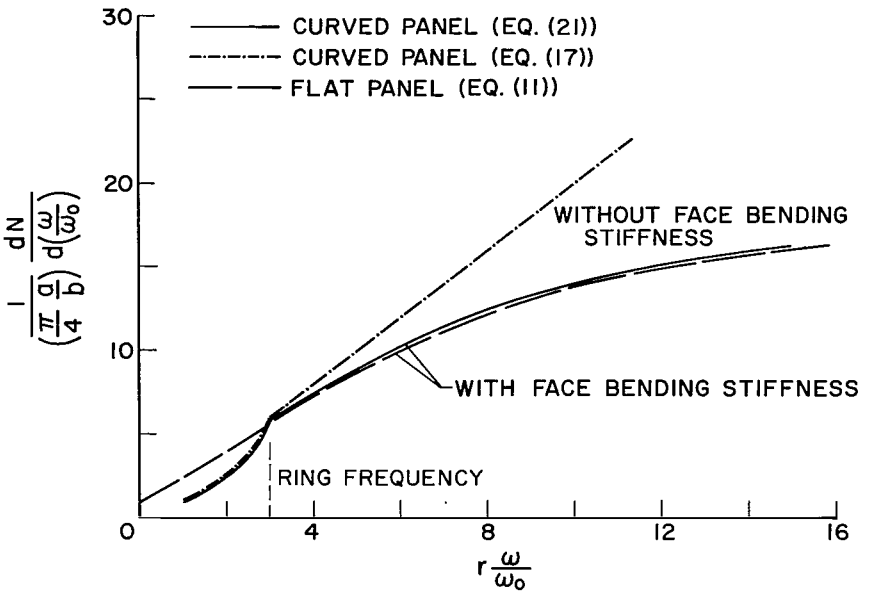

(a) rC = 3.0

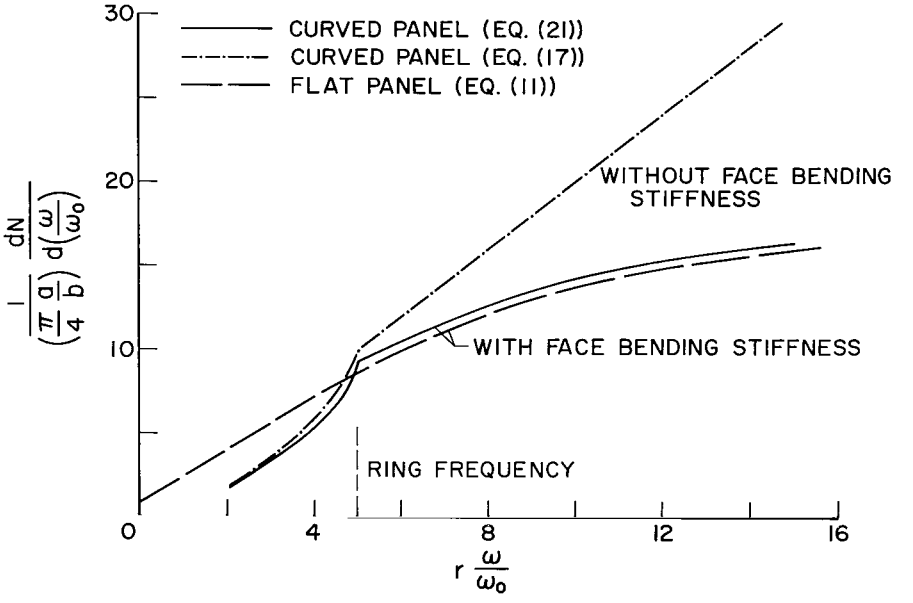

(b) rC = 5.0

Figure 9.- Combined effect of curvature and face bending stiffness on sandwich panel modal density; isotropic core; rotary inertia neglected; $t_f/h_c = 0.10$.

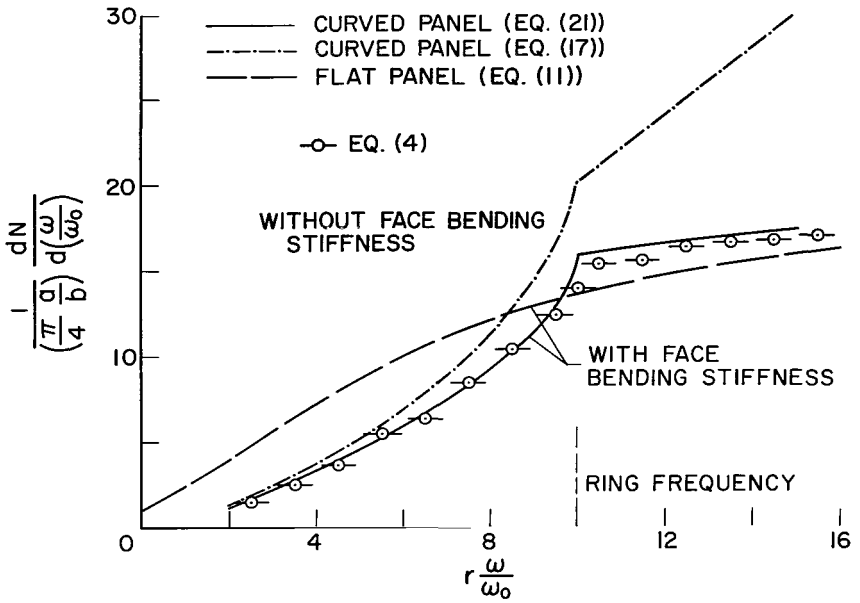

(c) rC = 10.0

Figure 9.- Concluded.

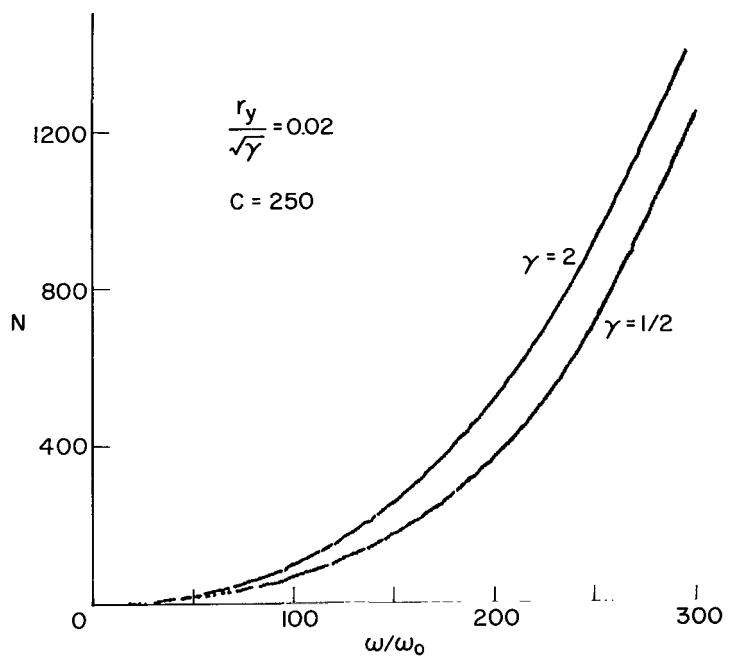

Figure 10.- Effect of core orthotropy on cumulative number of modes for a cylindrically curved panel as predicted by equation (26); rotary inertia and face bending stiffness neglected; a/b = 1.27.

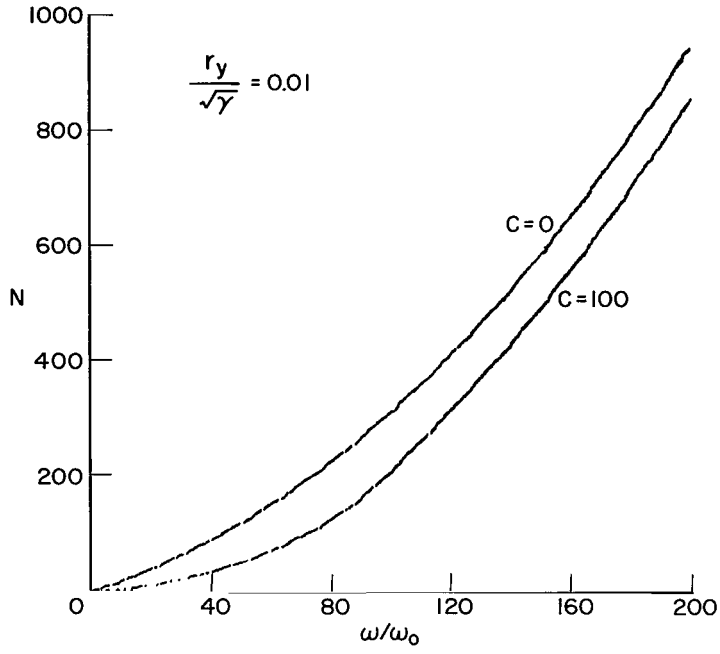

(a) Exact; equation (26).

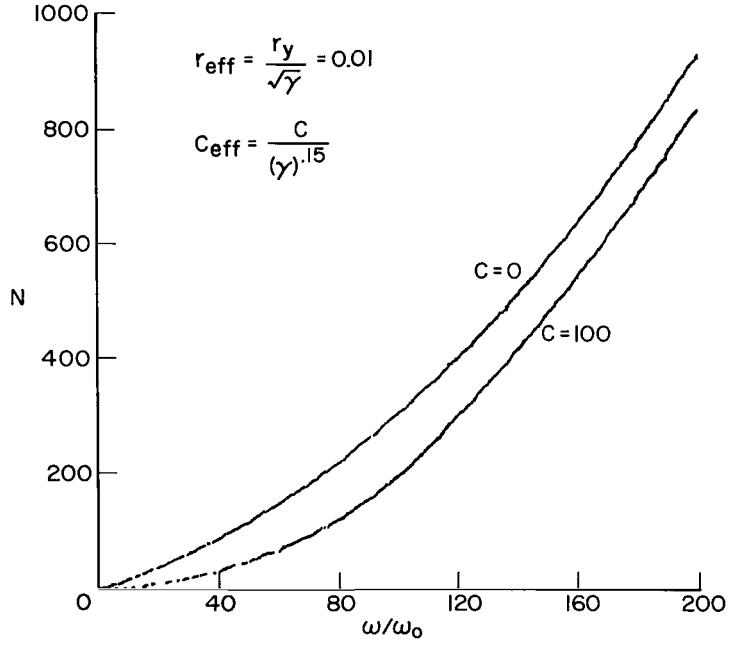

(b) Empirical; equation (27).

Figure 11.- Comparison of cumulative number of modes for sandwich panels as predicted by exact and empirical frequency equations; rotary inertia and face bending stiffness neglected; a/b = 2.55, γ = 0.5.

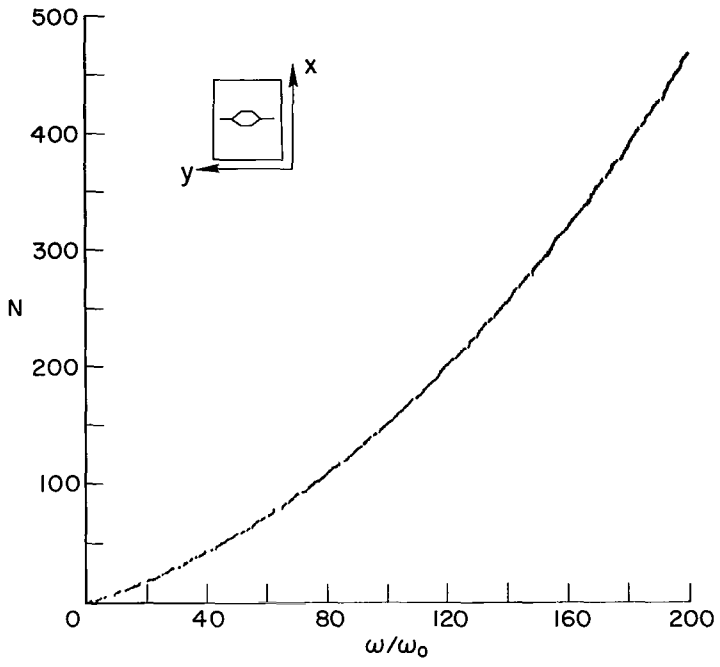

(a) $\gamma = 0.5$

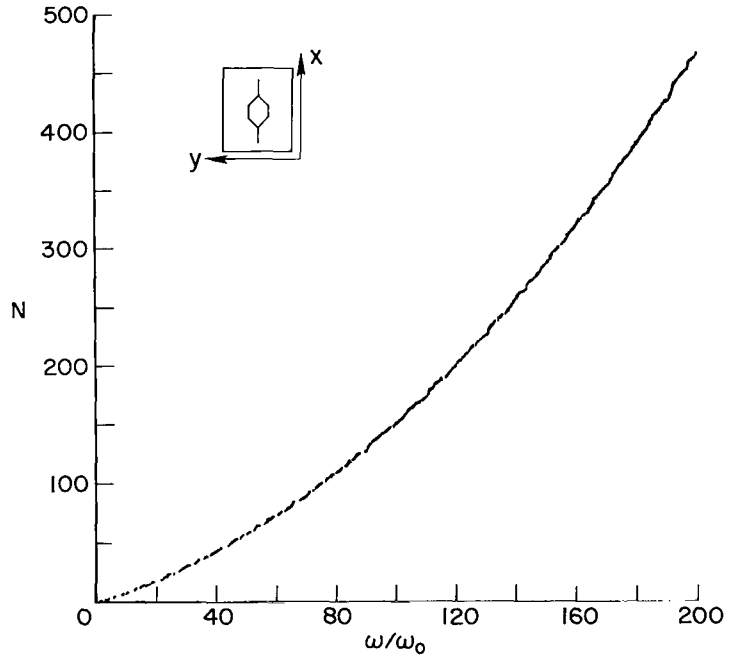

(b) $\gamma = 2.0$

Figure 12.- Comparison of cumulative number of modes for two flat sandwich panels which have orthotropic cores differing in orientation by 90°; rotary inertia and face bending stiffness neglected; a/b = 1.27; $r_y/\sqrt{\gamma} = 0.01$.

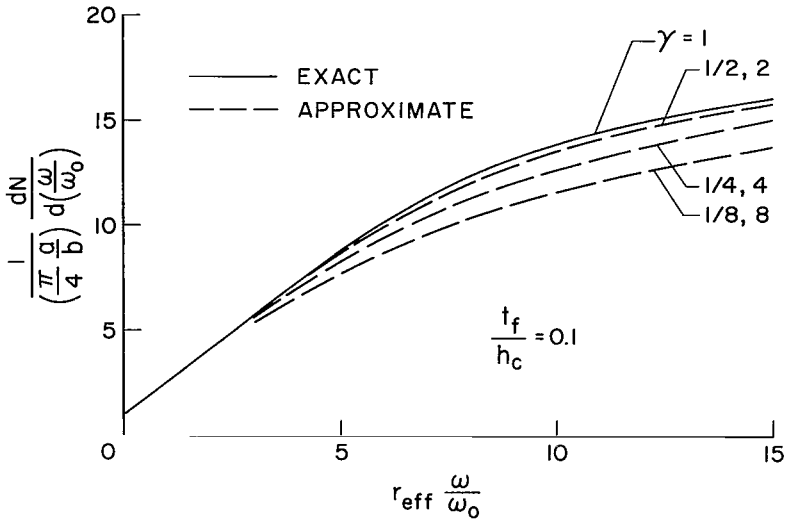

Figure 13.- Combined effect of orthotropic core shear moduli and face bending stiffness on the modal density of a flat sandwich panel; rotary inertia neglected.

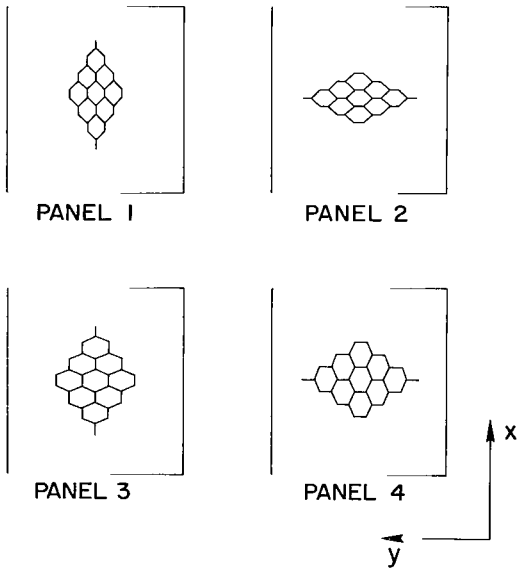

Figure 14.- Core geometries and orientations. (Core cell size is exaggerated.)

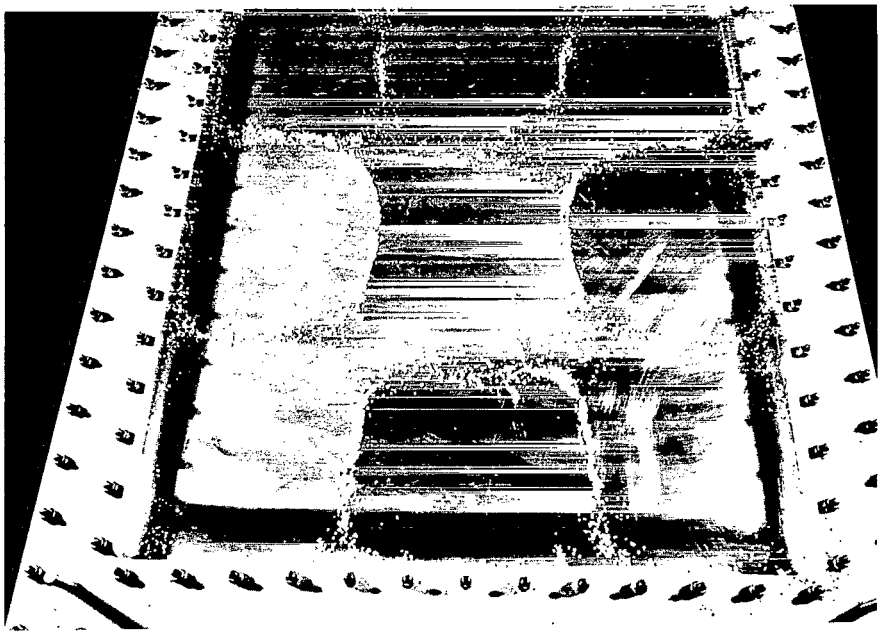

A-41047

(a) Mode (3, 3) - 1260 Hz.

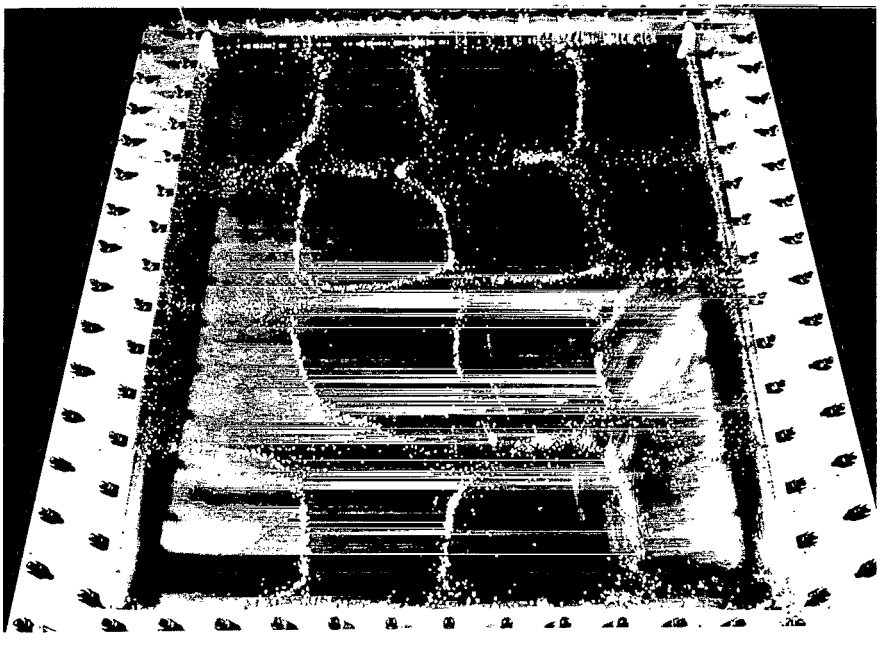

A-41046

(b) Mode (4, 4) - 1780 Hz.

Figure 15.- Some Chladni figures on panel 4 showing modes (m, n).

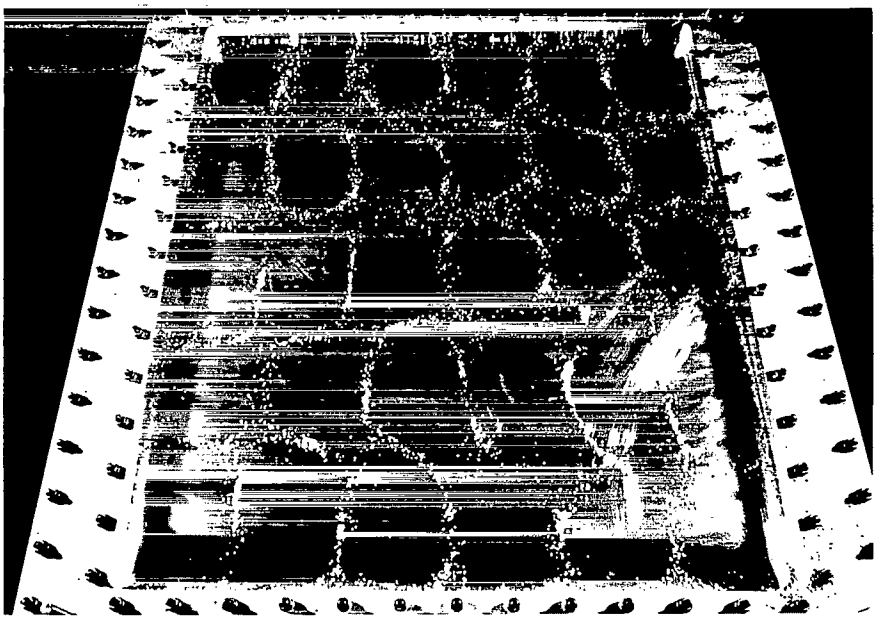

A-41050

(c) Mode (5, 6) - 2630 Hz.

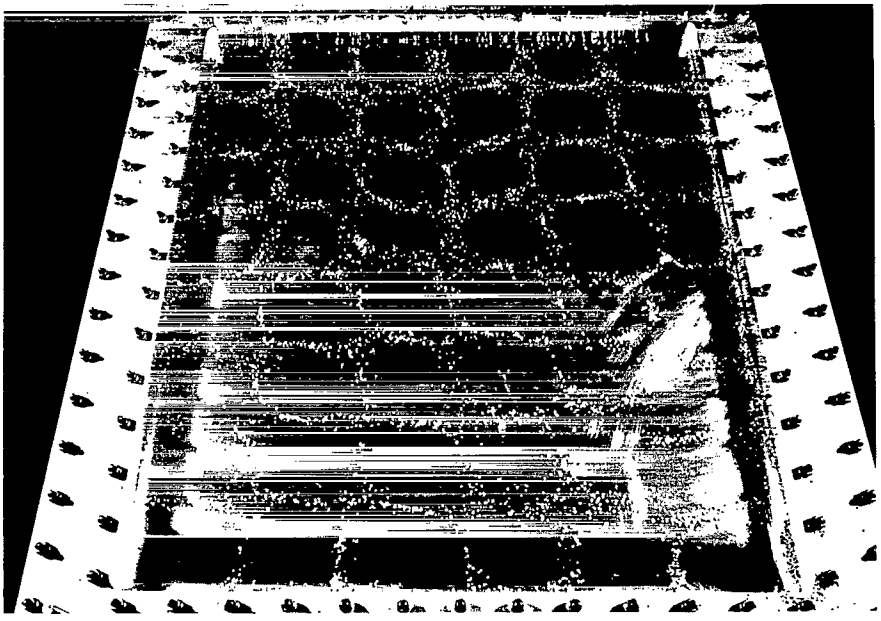

A-41051

(d) Mode (8, 6) - 3240 Hz.

Figure 15.- Concluded.

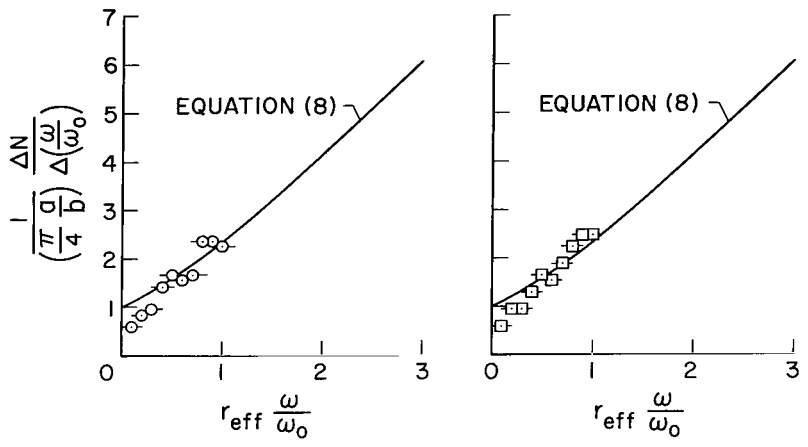

(a) Panel 1. (b) Panel 2.

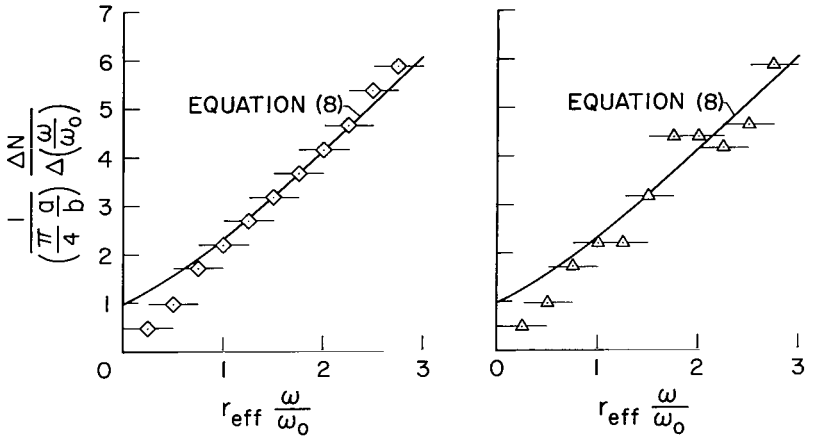

(c) Panel 3. (d) Panel 4.

Figure 16.- Comparison of theoretical and experimental modal densities.

NASA-Langley, 1970 —— 32 A-3106

"The aeronautical and space activities of the United States shall be conducted so as to contribute . . . to the expansion of human knowledge of phenomena in the atmosphere and space. The Administration shall provide for the widest practicable and appropriate dissemination of information concerning its activities and the results thereof."

—NATIONAL AERONAUTICS AND SPACE ACT OF 1958

NASA SCIENTIFIC AND TECHNICAL PUBLICATIONS

TECHNICAL REPORTS: Scientific and technical information considered important, complete, and a lasting contribution to existing knowledge.

TECHNICAL NOTES: Information less broad in scope but nevertheless of importance as a contribution to existing knowledge.

TECHNICAL MEMORANDUMS: Information receiving limited distribution because of preliminary data, security classification, or other reasons.

CONTRACTOR REPORTS: Scientific and technical information generated under a NASA contract or grant and considered an important contribution to existing knowledge.

TECHNICAL TRANSLATIONS: Information published in a foreign language considered to merit NASA distribution in English.

SPECIAL PUBLICATIONS: Information derived from or of value to NASA activities. Publications include conference proceedings, monographs, data compilations, handbooks, sourcebooks, and special bibliographies.

TECHNOLOGY UTILIZATION PUBLICATIONS: Information on technology used by NASA that may be of particular interest in commercial and other non-aerospace applications. Publications include Tech Briefs, Technology Utilization Reports and Notes, and Technology Surveys.

Details on the availability of these publications may be obtained from:

SCIENTIFIC AND TECHNICAL INFORMATION DIVISION

NATIONAL AERONAUTICS AND SPACE ADMINISTRATION

Washington, D.C. 20546